

Response Letter

Dear editors,

Dear reviewers,

Much appreciation for your valuable comments and suggestions. In the revised manuscript we incorporated the suggested changes according to our response in the open discussion. Please find below a point by point response on all your comments followed by changes tracked version of the revised manuscript.

We hope that the revised manuscript will be satisfactory to be published in Biogeosciences.

Sincerely,

Andreas Hartmann on behalf of the co-authors.

Referee #1

We thank referee #1 again for her/his positive opinion and valuable remarks. In the revised manuscript we will included

- Information about the size of the study site (lines 89 and 98 in the revised manuscript).
- Elaborations on the laboratory methods to analyse of DOC and DIN (lines 114-127 in the revised manuscript).
- an outlook on how further field campaigns could improve the understanding of DOC and DIN dynamics, especially during peak flows (lines 369-375 in the revised manuscript).

Furthermore, all technical comments were applied in the revised manuscript (also see changes tracked version below):

- “lime-stone” was changed to “limestone”.
- “stream Sects.” Was changed to “stream sections”.
- The unnecessary comma was removed.
- The unnecessary “in” was removed.

Referee #2

We thank referee #2 for her/his positive opinion and valuable remarks. Please find below our response and revisions according her/his general and detailed/technical comments:

General comment 1: *a few details and precisions would be worth to add especially about the processes that are dominant in this systems (see below comments on LULC, fast/slow components, “N saturated systems” definition. . .)*

Response: More details to these points are provided in the revised version of the manuscript. Please see our response to the detailed/technical comments below.

General comment 2: *a few details and precisions would be worth to add especially about (...) the procedure in model recalibration (so called “adaptation” by the authors) and underlying hypotheses the unmodified hydrological response to disturbance regarding the respective flow paths of DOC and DIN exports.*

Response: We will elaborate the adaption procedure in more detail in the revised version of the manuscript (lines 226-228 in the revised manuscript, see also our response to detailed/technical comment 7). Concerning the underlying hypotheses about the hydrological response on the disturbance please refer to our responses to detailed/technical comments 5 and 19.

Detailed/technical comment 1: *p. 11989 L.25: Please explain what is meant by “N saturated systems”?*

Response: Generally, pristine forest ecosystems are defined as N limited systems due to the marginal deposition of N and the lacking supply from weathering (i.e. growth is limited by the absence of available N). The substantial economic and population growth in Europe and North America since the 1950s has caused extensive emissions of nitrogen oxides (NO_x) into the atmosphere. In addition, the intensification of agriculture emitted large quantities of ammonia (NH₃). Subsequently, elevated deposition of airborne N increases the amount of N within the forest ecosystems readily available for prominent biogeochemical processes like tree growth, mineralization of organic carbon and nitrification. Sustained elevated N deposition raises the N status of these ecosystems until N saturation. Nitrogen saturation of forests is reached when the availability of inorganic nitrogen exceeds demand by plants and microbes and causes elevated NO₃ concentrations (in surface waters), elevated NO₃ leaching, soil acidification and nutrient imbalances of plants. We extended the introduction of the revised manuscript to clarify on this (lines 58-59 in the revised manuscript).

Detailed/technical comment 2: *p. 11990 L. 20-21: So the underlying hypothesis is that if the behavior changes, (which would be revealed if the model fails to reproduce behavior after the storms) it would be due to changes in DOC and DIC inputs in the hydrological system only? As shown by the “adaptation” procedure (p. 11996, L. 15-16) no changes are assumed in the transfer processes: neither in flow paths (and while total flow could be unchanged, its relative contributors may be) nor in transit times along these flow paths because only hydrochemical parameters are readjusted? No transformation is assumed to occur along the flow paths (only before mobilization by water)? Additional discussion or argumentations about this point would be appreciated.*

Response: Referee #2 is right – a disturbance on the forest cover can affect more than the DOC and DIN mobilisation and transport. There are possible impacts on hydrological processes such as a decrease of transpiration or an increase of groundwater recharge. But due to the karstic characteristics of our study site this increase may be minor compared to the typically high karstic recharge rates (see also our response on detailed/technical comments 5 and 19). In Figure 2e we show that there is no obvious change in the variability of discharge before and after the disturbance. Admittedly, internal processes may change but if so, these changes are not identifiable by observed discharges alone. A better understanding about changes of system internal hydrological processes could only be derived by system internal observations, which were not available for this study. This information, as well as a more detailed discussion on possible changes of hydrological processes was added to the discussion (lines 369-375 in the revised manuscript, see also our response to detailed/technical comment 14).

Detailed/technical comment 3: p. 19911 L.13: “Hydromorphic”

Response: Corrected (see changes tracked version below).

Detailed/technical comment 4: p. 11991 L.1 to 5: *Is there any difference in the Land Use/land cover between the hillslopes and the plateau?*

Response: Both plateau and slopes are mainly covered by forest. Norway spruce (*Picea abies* L. Karst.) interspersed with beech (*Fagus sylvatica* L.) was planted after a clear cut around the year 1910. The vegetation at the slopes is dominated by semi-natural mixed mountain forest with beech (*Fagus sylvatica*) as the dominant species, Norway spruce (*P. abies*), maple (*Acer pseudoplatanus*), and ash (*Fraxinus excelsior*). If necessary, bark beetle abatement measures (i.e. salvage of trees infested by bark beetle and/or affected by wind) were conducted at the plateau since the installation of the LTER site in 1993. At the slopes no forest management has been conducted since the implementation of the National Park. We added this information to the study site description (lines 100-106 in the revised manuscript).

Detailed/technical comment 5: p. 11992 section 2.2.: *So the DOC sources would be unimpacted? Could the impact be hidden by soil buffering effect or variations in the hydrological connectivity (e.g.: if less ET and less interception would induce more infiltration and deeper flowpaths through layers that would be poorer in DOC?)*

Response: In the short-term forest disturbance has a substantial positive impact on DOC production via the large input of dead organic matter and altered soil climate. In the long run organic carbon input to the disturbed ecosystem – as important DOC source – decreases due to the decreasing litter input. However, as most of the produced DOC is processed by microorganisms and respired back to atmosphere as CO₂, the effect of forest disturbance is superior for NO₃ than for DOC sources. Concerning DOC leaching, the disturbance effect seems to be the net outcome of increased DOC leaching due to increased and accelerated seepage fluxes and its highly efficient adsorption on mineral soil compartments within soil. Surprisingly, Figure 2b shows no substantial effect of forest disturbance on DOC leaching. Thus, more detailed analysis of existing data and high temporal-resolution sampling have to be undertaken to elucidate the effect of forest disturbance on DOC leaching within the studied ecosystem. We expanded the discussion of the revised manuscript by

these interesting points (lines 369-375 in the revised manuscript, see also our response on detailed/technical comment 19).

Detailed/technical comment 6: *p.11993 Table 1 does not describe all the variables: $R_{diff,i}$; $R_{conc,i}$; $Q_{gw,i}$ and Z are missing.*

Response: Table 1 was only meant to provide a complete list of model parameters, their description, units, ranges, and optimised values. Simulated fluxes as $R_{diff,i}$, $R_{conc,i}$, or $Q_{gw,i}$ are variables that change over time; they do not have upper or lower ranges that are used for calibration. We therefore decided defining them within the methods description instead of another table.

Detailed/technical comment 7: *p.11996 L.4 : What kind of threshold or rules are used to characterize the performance as significantly reduced or not? Is it a statistical significance test? If so please cite which one.*

Response: We considered deviation of performance as significantly different when a component of KGE (correlation, bias, or variability) fell below or above its pre-disturbance variability as indicated by the whiskers of the calibration/validation periods in Figure 6. We added this important information to subsection 3.3 of the revised version of the manuscript and to the caption of Figure 6 (lines 226-228 and Figure 6 in the revised manuscript, see also our response to detailed/technical comment 7).

Detailed/technical comment 8: *p.11996 L9.: At this stage it would be worth to know what are “adapted” and “non adapted “ simulations, it comes just after but these sentences could maybe be rear-ranged so that the reader immediately knows it?*

Response: The mentioning of adapted and non-adapted simulation was rearranged accordingly (lines 223-224 in the revised manuscript). Thanks for this helpful advice.

Detailed/technical comment 9: *p. 11996 L. 25: It is unclear for me if these times are mean transit times within the compartment or mean residence times in it as the compartment is part of the system. . .?*

Response: Thanks to referee #2 for this clarifying comment. As we assume complete and instantaneous mixing with each model storage (soil, epikarst groundwater) at each compartment, the time that we refer to as “mean transit time” of a model compartment is the time the virtual tracer needs to pass through the particular storage. If we would have only one storage for each compartment, our mean transit time would be similar to the mean residence time of the compartment but since we look at series of different storages that exchange virtual tracer within and between the model compartments we the term “transit time” more appropriate. A clarification was added subsection 3.4 in the revised version of the manuscript (lines 241-244 in the revised manuscript).

Detailed/technical comment 10: *p. 11997 L. 1-2: Are slow and fast flows associated to the epikarst and the groundwater or do both contributions have a fast and a slow component?*

Response: Both epikarst and groundwater have slow and fast storage components as defined by their distribution of storage coefficients in Eqs (A6) and (A12). A clarification was added to subsection 3.4 (lines 240-241 in the revised manuscript).

Detailed/technical comment 11: p. 11997 L.5-7: *How long is the pulse in the second virtual tracer simulation?*

Response: The disturbance period lasted from May 1st, 2007, to September 30th, 2011. This is mentioned in the results section but it was not clearly stated that the same period was also used to define the length of the second virtual tracer injection. The missing information was added to the revised version of the manuscript (lines 248-249 in the revised manuscript).

Detailed/technical comment 12: p. 11997 L.14: *Could you explain what a “natural equilibrium concentration” is? The concept of production constant is different from a concentration which results from production/consumption rates but also from export rates and volumes in each component. What does it mean when this concentration is negative?*

Response: The term “natural equilibrium concentration” is not chosen well at least for DOC and DIN. As explained in subsection 3.1.2, we assume net production rates that result in typical DOC/DIN concentrations, which are variable over the model compartments and constant over time (DOC) or constant over the model compartments and variable over time (DIN). Negative values, as found for DIN, indicate that during some periods of the year all DIN is consumed by plants or soil organisms. But as also shown in Table 1, an amplitude A_{DIN} of the seasonal DIN production of 3.36 will mg/L also result in positive values of DIN production at another period of the year. In the revised manuscript, we now consistently use the term production rate over the entire manuscript (see changes tracked version below). We also clarified the meaning of negative DIN values in the discussion (lines 328-330 in the revised manuscript).

Detailed/technical comment 13: p. 11997 L. 22-23: *Do you have any hypothesis to explain the higher stability of the second sample? Is there any difference in climatic conditions between both samples?*

Response: Thanks for this valuable comment. Since both samples' time span is only 4 years and the resolution of the hydrochemical variables (SO₄, DOC and DIN) is rather low, differences between the two samples may mostly be due to their rough resolution. Since both samples are bootstrapped from the same period, climatic conditions are the same. A clarification was added to subsection 4.1 of the revised manuscript (lines 304-308 in the revised manuscript).

Detailed/technical comment 14: p. 11998 L.4: *As DIN is diluted during peak flow and peak flows are underestimated, wouldn't this contribute to an overestimation of DIN? However, is NH₄⁺ sometimes monitored during peak flows?*

Response: This is a good point. Indeed, an under-estimation of peak flows would go along with a weaker dilution of DIN concentrations. However, since the model is calibrated by discharge and solute concentration, the resulting parameter sets may compensate for this, for instance by a reduced the DIN production parameter. Since the resolution of DIN observations is quite low compared to the resolution of the discharge observations we cannot evaluate the model's behaviour

during events in more detail. High-resolution sampling of DIN (and NH₄⁺) may provide some more insight, but such data was unfortunately not available for our study. We added some discussion on calibration related compensatory effects on simulated solute concentrations in the revised version of the manuscript (lines 372-375 in the revised manuscript, see also our response to detailed/technical comment 2).

Detailed/technical comment 15: p. 11998 L. 24: “more than 2 times 2 mg/l that the pre-disturbance value” this sentence is not fully clear, is it? Please rephrase.

Response: The sentence will be rephrased in the revised version of the manuscript (see changes tracked version below).

Detailed/technical comment 16: p. 11999 L. 2: How could this phase shift be related to hydrological changes (e.g. inrelative contribution or mean transit times of the components)?

Response: This small shift towards earlier DIN production may be due to a decreased shadowing effect due to the windthrow. Snow melt would initiate earlier going along with an earlier DIN production and leaching. Hence, an earlier snowmelt may also be visible in the discharge observations. However, due to the rather slow melting rates, most of the melting water will slowly/diffusively enter the groundwater system rather than flowing rapidly through the karst conduits. Therefore, a slightly earlier beginning of snowmelt may not be visible at the system outlet due to the slow reaction of the groundwater storage (also see our response to detailed/technical comment 19). We added some more discussion on possible (non-visible) changes on the hydrological behaviour of the system in the revised manuscript (lines 369-372 in the revised manuscript).

Detailed/technical comment 17: p. 11999 L. 17: “The soil” please remove comma. Aren’t these large storage capacity values related to the short storage constants? (There is probably some correlation between these parameters?)

Response: Thanks for this valuable comment. In the revised manuscript, we specified our elaborations about the relatively high storage capacities of the soil and the epikarst by mentioning possible parameter interactions between their storage capacities and storage coefficients (lines 313-314 in the revised manuscript). The comma was removed, too.

Detailed/technical comment 18: p. 12000 L. 9-10: How was the “realism” of hydrochemical values appreciated? Were they compared to measurements? P_DIN is homogeneous to a concentration and not to a rate so I wonder how realistic is a negative value?

Response: This was an unfortunate formulation. In the revised manuscript we rephrased it to “A DOC production parameter P_DOC of ~1.6-1.8 mg/L resulted in realistic simulated concentrations at the weir.” (lines 324-325 in the revised manuscript). About an elaboration of the meaning of negative P_DIN values please refer to our response on detailed/technical comment 12.

Detailed/technical comment 19: p. 12001 L. 7: *Why total flow doesn't vary? If the loss of trees is enough to change N uptake I am surprised that it is not enough to change transpiration. Moreover, there is at least some changes in the dynamic of flow: p. 12002 L.26.*

Response: This is a very good question. Our study site is composed of karstified dolostone resulting in strong subsurface heterogeneity. As a consequence there is an interplay of fast preferential flow and low diffuse flow through the subsurface resulting in a very dynamic hydrological behaviour at the outlet (see for instance Fig 4). When preferential flow paths activate during wet conditions large parts of the flow can bypass the soil resulting in generally lower evaporation rates in karst systems (Hartmann et al., 2014, 2015). Therefore, hydrological impacts of windthrow on karst systems may not be as pronounced as in non-karstic domains because a large fraction of the infiltration during high flow periods will not be available for transpiration anyway (see also our response on detailed/technical comment 5). However, during medium and low flow conditions, most of the water passes the soil and windthrow related changes of transpiration may alter the hydrological behaviour, as they also alter DIN production. Decreasing differences of pre-disturbance and wind disturbance DIN concentrations with increasing discharge (Fig. 2d) may support this argumentation. We added these points to the discussion of the revised manuscript (lines 369-375 in the revised manuscript).

Detailed/technical comment 20: p. 12003 L. 10: *What were the dominant ranges of water ages in groundwater?*

Response: Previous studies (Kralik et al., 2009) indicated water ages of weeks to months at the weir (by Oxygen-18 analysis), while they found fast transit times of days (artificial tracer experiments) and old waters of several years (CFCs, SF6 dating) at small individual springs within the study area. Hence there is some indication that the mean transit times found by the virtual tracer experiment reflect at least the behaviour of the sub-catchment drained by the weir, which can be regarded as more dominant than the rather local observations at the springs. This information was added to the revised version of the manuscript (lines 405-412 in the revised manuscript).

Detailed/technical comment 21 Figure 6: *please correct in the legend "observed" and "comparison" p. 12024*

Response: the legend was corrected.

Detailed/technical comment 22: Figure 7: *please correct in the legend "scenario 1", "scenario 2" and "variation" p.*

Response: the legend was corrected.

Detailed/technical comment 23: Figure 8: *please correct in the legend "groundwater", "infinite virtual", and "starting".*

Response: the legend was corrected.

Next page: Revised manuscript with changes tracked

1 **Model aided quantification of dissolved carbon and**
2 **nitrogen release after windthrow disturbance in an Austrian**
3 **karst system**

4
5 **A. Hartmann^{1,2}, J. Kobler³, M. Kralik³, T. Dirnböck³, F. Humer³ and M. Weiler¹**

6 [1] ~~Faculty of Environment and Natural Resources~~~~Institute of Hydrology~~, Freiburg University,
7 Germany

8 [2] Department of Civil Engineering, University of Bristol, UK

9 [3] Environment Agency Austria, Vienna, Austria

10 Correspondence to: A. Hartmann (andreas.hartmann@hydrology.uni-freiburg.de)

11

12 **Abstract**

13 Karst systems are important for drinking water supply. Future climate projections indicate
14 increasing temperature and a higher frequency of strong weather events. Both will influence
15 the availability and quality of water provided from karst regions. Forest disturbances such as
16 windthrow can disrupt ecosystem cycles and cause pronounced nutrient losses from the
17 ecosystems. In this study, we consider the time period before and after the wind disturbance
18 period (2007/08) to identify impacts on DIN (dissolved inorganic nitrogen) and DOC (dissolved
19 organic carbon) with a process-based flow and solute transport simulation model. Calibrated
20 and validated before the disturbance the model disregards the forest disturbance and its
21 consequences on DIN and DOC production and leaching. It can therefore be used as a base-line
22 for the undisturbed system and as a tool for the quantification of additional nutrient production.
23 Our results indicate that the forest disturbance by windthrow results in a significant increase of
24 DIN production lasting ~3.7 years and exceeding the pre-disturbance average by 2.7 kg/ha/a
25 corresponding to an increase of 53%. There were no significant changes of DOC
26 concentrations. With simulated transit time distributions we show that the impact on DIN
27 travels through the hydrological system within some months. But a small fraction of the system
28 outflow (<5%) exceeds mean transit times of >1 year.

29 1 Introduction

30 Karst systems contribute around 50% to Austria's drinking water supply (COST, 1995). Karst
31 develops due to the dissolvability of carbonate rock (Ford and Williams, 2007) and it results in
32 strong heterogeneity of subsurface flow and storage characteristics (Bakalowicz, 2005). The
33 resulting complex hydrological behavior requires adapted field investigation techniques
34 (Goldscheider and Drew, 2007). Future climate trajectories indicate increasing temperature
35 (Christensen et al., 2007) and a higher frequency of hydrological extremes (Dai, 2012;
36 Hirabayashi et al., 2013). Both will influence the availability and quality of water provided
37 from karst regions because temperature triggers numerous biogeochemical processes and fast
38 throughflow water has a disproportional effect upon water quality. Also forest disturbances
39 (windthrows, insect infestations, droughts) pose a threat on water quality through the
40 mobilization of potential pollutants and these disturbances are likely to increase in future
41 (Johnson et al., 2010; Seidl et al., 2014).

42 A way to quantify the impact of changes in climatic boundary conditions on the hydrological
43 cycle are simulation models. Special model structures have to be applied for karst regions to
44 account for their particular hydrological behavior (Hartmann et al., 2014a). A range of models
45 of varying complexity is available from the literature, that deal with the karstic heterogeneity,
46 such as groundwater flow in the rock fracture matrix and dissolution conduits (Jourde et al.,
47 2015; Kordilla et al., 2012), varying recharge areas (Hartmann et al., 2013a; Le Moine et al.,
48 2008) or preferential recharge by cracks in the soil or fractured rock outcrops (Rimmer and
49 Salinger, 2006; Tritz et al., 2011).

50 Nitrate and dissolved organic carbon (DOC) have both been considered in drinking water
51 directives and water preparation processes (Gough et al., 2014; Mikkelsen et al., 2013; Tissier
52 et al., 2013; Weishaar et al., 2003). Though nitrate pollution of drinking water is usually
53 attributed to fertilization of crops and grassland, an excess input of atmospheric nitrogen (N)
54 from industry, traffic and agriculture into forests has caused reasonable nitrate losses from
55 forest areas (Butterbach-Bahl et al., 2011; Erisman and Vries, 2000; Gundersen et al., 2006;
56 Kiese et al., 2011). The Northern Limestone Alps area is exposed to particularly high nitrogen
57 deposition (Rogora et al., 2006) and nitrate leaching occurs in increased rates (Jost et al., 2010).
58 Apart from this, forest disturbances such as windthrow and insect outbreaks disrupt the N cycle
59 and cause pronounced nitrate losses from the soils, at least in N saturated systems, [that received](#)
60 [elevated N deposition due to elevated NOx in the atmosphere](#) (Bernal et al., 2012; Griffin et al.,

61 2011; Huber, 2005). Contrary to N deposition, atmospheric deposition of DOC is low (Lindroos
62 et al., 2008) and thus has not been identified as major driver of DOC leaching from subsoil
63 (Fröberg et al., 2007; Kaiser and Kalbitz, 2012; Verstraeten et al., 2014). Moreover, studies
64 show contrasting results but point to increased DOC (TOC) leaching from soil and catchments
65 after forest disturbances (Huber et al., 2004; Löfgren et al., 2014; Meyer et al., 1983; Mikkelsen
66 et al., 2013; Wu et al., 2014).

67 While many studies identify N and DOC as source of contamination in karst systems (Einsiedl
68 et al., 2005; Jost et al., 2010; Katz et al., 2001, 2004; Tissier et al., 2013) or provide static
69 vulnerability maps (Andreo et al., 2008; Doerfliger et al., 1999), only very few studies use
70 models to quantify the temporal behavior of a contamination through the systems (Butscher and
71 Huggenberger, 2008). Some studies use N and DOC to better understand karst processes
72 (Charlier et al., 2012; Mahler and Garner, 2009; Pinault et al., 2001) or for advanced karst
73 model calibration (Hartmann et al., 2013b, 2014b) but from our knowledge there are no
74 applications of such approaches to quantify the drainage processes of N and DOC, and
75 particularly so after strong impacts on ecosystems (e.g. windthrow) that release reasonable
76 amount of nitrate from the forest soils.

77 In this study, we consider the time period before and after storm Kyrill (early 2007) and several
78 other storm events (2008) that hit Middle Europe. The storms, from now on referred to as the
79 wind disturbance period, caused strong damage to the forests in our study area, a dolomite karst
80 system. We apply a new type of semi-distributed model that considers the spatial heterogeneity
81 of the karst system by distribution functions. We aimed at comparing the hydrological and
82 hydrochemical behavior (DOC, DIN) of the system before and during the wind disturbing
83 period. In particular, we wanted to understand if and how DOC and DIN input to the
84 hydrological system changed by the impact of the storms. Furthermore, we used virtual tracer
85 experiments to create transit time distributions that expressed how the impact of the storms
86 propagated through the variable dynamic flow paths of the karst system. This allowed us to
87 assess the vulnerability of the karst catchment to such impacts.

88 **2 Study site**

89 The study site LTER Zöbelboden is located in the northern part of the national park “Kalkalpen”
90 (Figure 1 ~~Figure 1~~). Its altitude ranges from 550 m to 956 m ASL and its area is ~5.7 km². Mean
91 monthly temperature varies from -1 °C in January to 15.5 °C in August. The average
92 temperature is 7.2 °C (at 900 m ASL). Annual precipitation ranges from 1,500 to 1,800 mm

93 and snow accumulates commonly between October and May with an average duration of about
94 4 months. The mean N deposition in bulk precipitation between 1993 and 2006 was 18.7 kg N
95 ha⁻¹.yr⁻¹, out of which 15.3 kg N (82%) was inorganic (approximately half as NO₃⁻-N and half
96 as NH₄⁺-N) (Jost et al., 2011). Due to the dominating dolomite, the catchment is not as heavily
97 karstified as limes-tone karst systems, but shows typical karst features such as conduits and
98 sink holes (Jost et al., 2010). The site can be split into steep slopes (30-70°, 550-850 m ASL)
99 and a plateau (850-950 m ASL), with the plateau covering ~0.6 km². Chromic cambisols and
100 hydromorphic stagnosols with an average thickness of 50 cm and lithic and rendzic leptosols
101 with an average thickness of 12 cm can be found at the plateau and the slopes, respectively
102 (WRB, 2006). Both plateau and slopes are mainly covered by forest. Norway spruce (Picea
103 abies L. Karst.) interspersed with beech (Fagus sylvatica L.) was planted after a clear cut around
104 the year 1910. The vegetation at the slopes is dominated by semi-natural mixed mountain forest
105 with beech (Fagus sylvatica) as the dominant species, Norway spruce (P. abies), maple (Acer
106 pseudoplatanus), and ash (Fraxinus excelsior). At the slopes no forest management has been
107 conducted since the implementation of the National Park.

108 2.1 Available data

109 A 10 year record of input and output observations was available. Starting from the hydrological
110 year 2002/03 it envelops well the stormy period that began in January 2007. It included daily
111 rainfall measurements and stream discharge measurements from stream ~~section~~ sections 1 and
112 2 (Figure 1 ~~Figure 1~~). We obtained the discharge of the entire system with a simple topography
113 based up-scaling procedure that is described in more detail in (Hartmann et al., 2012a). Irregular
114 (weekly to monthly) observations of DOC, DIN and SO₄²⁻ concentrations are available for
115 precipitation and at weir 1. DOC (entire study period), NO₃⁻, SO₄²⁻ and NH₄⁺ (since January
116 2010) samples were filtered (MILLIPOR HTTP04700 (0.4 µm) (Millipor Corporation, USA))
117 with SM 16249 (Sartorius AG, Germany) (xxxx-2009) and SM 16201/19/20 (Sartorius AG,
118 Germany) (2009-xxxx). NH₄⁺ concentrations were measured after filtering by
119 spectrophotometry (Milton Roy Spectronic 1201 (Thermo Fisher Scientific Inc., USA). Weekly
120 DOC, SO₄²⁻ and NO₃⁻ samples were pooled to provide volume weighted bi-weekly (until March
121 2009) and monthly (thereafter) samples. DOC samples were acidified with 0.5 ml HCl 25%.
122 All samples were kept at 4°C until analyses. NO₃⁻ and SO₄²⁻ concentrations were determined
123 by ion chromatography with conductivity detection (Bulk precipitation: 2002-2009: Dionex
124 ICS DX 500 (Dionex Corp., USA); 2010-xxxx: Dionex ICS 3000 (Dionex Corp., USA);

Formatiert: Tiefgestellt
Formatiert: Hochgestellt
Formatiert: Tiefgestellt
Formatiert: Hochgestellt
Formatiert: Tiefgestellt
Formatiert: Hochgestellt
Formatiert: Tiefgestellt
Formatiert: Hochgestellt
Formatiert: Tiefgestellt
Formatiert: Hochgestellt
Formatiert: Tiefgestellt
Formatiert: Hochgestellt
Formatiert: Tiefgestellt
Formatiert: Hochgestellt
Formatiert: Tiefgestellt
Formatiert: Hochgestellt

125 Runoff: 2001-2002: Dionex ICS DX 500 (Dionex Corp., USA); 2002-2010: Metrohm ICS 7xx
126 (Deutsche METROHM GmbH & Co. KG, Germany)). DOC concentrations were measured
127 with a Maihak Tocor 100 (SICK MAIHAK GmbH, Germany) (1996-2007) and a CPN
128 TOC/DOC-Analyzer (Shimadzu Corp., Japan) (2007-2010). DIN input was then calculated as
129 the sum of NO_3^- -N and NH_4^+ -N. Since NH_4^+ is either transformed into NO_3^- or absorbed in the
130 soil NH_4^+ concentrations in runoff are very small or not detectable. Therefore we calculated
131 DIN outputs as NO_3^- -N. Additionally, irregular observations of snow water equivalent at the
132 plateau allowed for independent setup of the snow routines.

133 **2.2 Recent disturbances**

134 Kyrill in the year 2007 and some similarly strong storms that followed 2008 caused some major
135 windthrows as well as single tree damages. A windthrow disturbance of ~ 5 ha occurred
136 upstream of weir 1. Though no direct measurements exist as to the total extent of the windthrow
137 area we estimate that 5-10 % of the study site has been subject to windthrow (Kobler et al.,
138 2015). We did not observe a significant change in intra- and inter-annual variability of DOC
139 concentrations and discharge before and during the wind disturbance period (Figure 2Figure
140 2ae). Runoff concentrations of DIN showed clear responses to the disturbances. With the first
141 windthrow event it started to increase until 2008/09 and slowly decreased again in 2010/11
142 (Figure 2Figure 2c). Comparing DOC concentrations with discharge before and during the wind
143 disturbance period revealed a similar pattern. As shown by other studies on DOC mobilization
144 (e.g., Raymond and Saiers, 2010), a positive correlation between concentrations and discharge
145 (on log10 scale) occurred for DOC with concentrations up to 6 mg/l during high discharge
146 (similar to Frank et al., 2000). But there was no obvious difference between the pre-disturbance
147 period (Figure 2Figure 2b).

148 **3 Methods**

149 **3.1 The model**

150 **3.1.1 Model hydrodynamics**

151 The semi-distributed simulation model considers the variability of karst system properties by
152 statistical distribution functions spread over $Z=15$ model compartments (Figure 3Figure 3).
153 That way it simulates a range of variably dynamic pathways through the karst system. The
154 detailed equations of the model hydrodynamics are similar to its previous applications

155 (Hartmann et al., 2013a, 2013c, 2014b). They are described in the Appendix. Since in our case
 156 the model is used to simulate the discharge of the entire system and a weir within the system
 157 some small modifications had to be performed. Preceding studies showed that weir 1 (Figure
 158 1-Figure 1) receives its discharge partially from the epikarst and partially from the groundwater,
 159 reaching it partially as concentrated and partially as diffuse flow (Hartmann et al., 2012a).
 160 Consequently we derive its discharge Q_{weir} [l/s] by

$$Q_{weir}(t) = f_{Epi} \cdot \left[f_{Epi,conc} \cdot \sum_i^Z R_{conc,i}(t) + (1 - f_{Epi,conc}) \cdot \sum_i^Z R_{diff,i}(t) \right] + (1 - f_{Epi}) \cdot \left[f_{GW,conc} \cdot Q_{GW,Z}(t) + (1 - f_{GW,conc}) \cdot \sum_i^{Z-1} Q_{GW,i}(t) \right] \quad (1)$$

162 Where f_{Epi} is the fraction from the epikarst and $(1 - f_{Epi})$ the fraction from the groundwater. $f_{Epi,conc}$
 163 and $f_{GW,conc}$ represent the concentrated flow fractions of the epikarst and groundwater
 164 contributions, respectively. Table 1-Table 1 lists all model parameters including a short
 165 description.

166 3.1.2 Model solute transport

167 To model the non-conservative transport of DOC and, DIN and SO_4^{2-} , we equipped the model
 168 with solute transport routines. SO_4^{2-} was included as an additional calibration variable because
 169 it proved to be important to reduce model equifinality (Beven, 2006) by adding additional
 170 information about groundwater dynamics (Hartmann et al., 2013a, 2013b). The inclusion of
 171 these 3 solutes allowed for a more reliable estimation of model parameters (Hartmann et al.,
 172 2012b, 2013a) and, further on, the evaluation of possible changes in the dynamic of solute
 173 concentrations during the stormy period. For most of the model compartments they simply
 174 followed the assumption of complete mixing. But to represent net production and leaching of
 175 DOC and DIN in the soil, as well as dissolution of SO_4^{2-} in the rock matrix, additional processes
 176 were included in the model structure. Similar to preceding studies (Hartmann et al., 2013a,
 177 2014b) SO_4^{2-} dissolution $G_{SO_4,i}$ [mg/l] for compartment i is calculated by:

$$G_{SO_4,i} = G_{max,SO_4} \cdot \left(\frac{Z - i + 1}{Z} \right)^{a_{Geo}} \quad (2)$$

179 where a_{Geo} [-] is another variability parameter and G_{max,SO_4} [mg/l] is the equilibrium
 180 concentration of SO_4^{2-} in the matrix. DOC is mostly mobilised at in the forest floor (Borken et
 181 al., 2011). Stored in the soil or diffusively and slowly passing downwards, large parts of the

182 DOC is absorbed or consumed by micro-organisms. But when lateral flow and concentrated
 183 infiltration increase net leaching of DOC increases as well. For that reason our DOC transport
 184 routine only provides water to the epikarst when it is saturated (Eq. 10) with increasing DOC
 185 net production toward the more dynamic model compartments (Figure 3). Its DOC
 186 concentration $P_{DOC,i}$ [mg/l] for each model compartment is found by:

$$187 \quad P_{DOC,i} = P_{DOC} \cdot \left(\frac{Z-i+1}{Z} \right)^{\frac{1}{a_{DOC}}} \quad (3)$$

188 where a_{DOC} [-] is the DOC variability constant and P_{DOC} [mg/l] is the DOC net production at
 189 soil compartment 1. Similar to other studies that assessed N input to a karst system (Pinault et
 190 al., 2001) we used a trigonometric series to assess the time variant net production of DIN, $P_{DIN,i}$
 191 [mg/l], to the soil:

$$192 \quad P_{DIN,i} = P_{DIN} + A_{DIN} \cdot \sin\left(\frac{365.25}{2\pi} \cdot (J_D + S_{PH,DIN})\right) \quad (4)$$

193 Here, P_{DIN} is the mean amount of dissolved inorganic N in the soil solution, while A_N [mg/l]
 194 and $S_{PH,DIN}$ [d] are the amplitude of the seasonal signal and the phase shift of seasonal DIN
 195 uptake (immobilisation by plants and soil organisms) and release (net DIN in the soil water)
 196 cycle, respectively. J_D is the Julian day of each calendar year. Due to its seasonal variation $P_{DIN,i}$
 197 can also be negative meaning that uptake of DIN takes place.

198 3.2 Model calibration and evaluation

199 With 14 model parameter that controlled the hydrodynamics and 7 parameters that allow for
 200 the non-conservative solute transport, the calibration of the model was a high-dimensional
 201 problem. For that reason we have chosen the Shuffled Complex Evolution Metropolis algorithm
 202 SCEM (Vrugt et al., 2003) that prove itself to be capable of exploring high dimensional
 203 optimization problems (Fenicia et al., 2014; Feyen et al., 2007; Vrugt et al., 2006). As
 204 performance measure we used the Kling-Gupta efficiency KGE (Gupta et al., 2009). For
 205 calibration, KGE was weighted equally among all solutes, 1/3 for the discharge of the entire
 206 system, and 2/3 for the discharge of weir 1 whose observations precision was regarded to be
 207 more reliable than the up-scaled discharge. KGE is defined as:

$$208 \quad KGE = 1 - \sqrt{(r-1)^2 + (\alpha-1)^2 + (\beta-1)^2} \quad (5)$$

209 with $\alpha = \frac{\sigma_s}{\sigma_o}$ and $\beta = \frac{\mu_s}{\mu_o}$ (6)

210 where r is the linear correlation coefficient between simulations and observations, μ_s/μ_o and
211 σ_s/σ_o are the means and standard deviations of simulations and observations, respectively. α
212 expresses the variability and β the bias.

213 To check for the stability of the calibrated parameters, we perform a split-sample test (Klemeš,
214 1986). Since the pre-disturbance time series was too short to be split into two equally long
215 periods, we perform a both-sided split-sample test by bootstrapping two independent 4-year
216 time series of observations (1st sample: discrete sampling of 50% of the values of each observed
217 time series, 2nd sample: remaining 50% of the observations). We calibrate our model with the
218 1st sample and evaluate it with the 2nd sample, and vice versa. A parameter set is regarded stable,
219 when the calibration with both samples yields similar parameter sets and their KGE concerning
220 discharge and the solutes does not reduce significantly when applying them on the other sample.

221 3.3 Change of hydrochemical behaviour with the stormy period

222 After the model evaluation, we use the different components of the KGE in Eqs. (5) and (6) to
223 explore the impacts of the storm disturbance period on the hydrochemical components.
224 Assuming that the model is able to predict to hydrochemical behaviour that prevailed without
225 the impact of the storms adapting the hydrochemical parameters of the model in Eqs. (3)-(4)
226 and analysing –the difference between the adapted hydrochemical simulations and the non-
227 adapted simulations will allow us to quantify the change of solute mass balance due to the storm
228 impact. We define the time span for our adaption as the time when the different components of
229 KGE exceed the range of their pre-disturbance variability. During this time period we further
230 use the time span of deviation to assess the duration of the impact and to compensate for the
231 apparent deviations by adapting the hydrochemical parameters ~~in Eqs. (3)-(4)~~. This is done
232 twice, once by manual adaption and another time using an automatic calibration scheme. Their
233 new values will indicate changes of the seasonality, production or inter-annual variations.

234 3.4 Transit time distributions

235 The signal of the storm impact will travel by various velocities and pathways through the karst
236 system. While fast flow paths and small storages will transport the signal rapidly to the system
237 outlet, slow pathways and large storages will delay and dilute the signal. Transit time

238 distributions indicate how fast surface impacts travel through the hydrological system. We
239 derive transit time distributions from the model by performing a virtual tracer experiment with
240 continuous injection over the entire catchment at the beginning of the impact of the stormy
241 period. When a model compartment reaches 50% of the tracer concentration is considered as
242 median transit time. The hereby-derived transit times will elaborate how the hydrological
243 system propagates the signal through the system including all slow and fast pathways as defined
244 by Eqs. (12) and (18). As for DIN and DOC we assume complete and instantaneous mixing
245 with each model storage (soil, epikarst, and groundwater) at each compartment, the time that
246 we refer to as “mean transit time” of a model compartment is the time the virtual tracer needs
247 to pass through the particular model storage. In combination with the fluxes that are provided
248 from each of the model compartments, it is possible to quantify the fractional contribution of
249 fast and slow flow paths, respectively. We will apply the virtual tracer from the previously
250 assessed beginning of the impact until the end of the time series to assess the transit time
251 distribution. In addition, we apply a second virtual tracer that also lasts only for the disturbance
252 period (as estimated in subsection 3.3) starts with the assessed beginning of the impact but ends
253 at the assessed end of the impact to evaluate the filter and retardation potential of the karst
254 system.

255 4 Results

256 4.1 Model performance

257 Table 1 shows the calibrated parameters for the two samples. They indicate a thick soil
258 and a relatively thin epikarst. The dynamics expressed by the storage constants indicate days
259 and weeks for the conduits (model compartment $i=Z$) and the epikarst, respectively. The
260 distribution coefficient of the groundwater is larger than the soil/epikarst storage constant. For
261 DOC and DIN there are a natural production rates equilibrium concentrations of 1.6-1.8 mg/l
262 and -1.35-0.1 mg/l, respectively. The DOC distribution coefficient is between 0.9 and 1.1. The
263 phase shift and amplitude for DIN showed that there is a seasonal variation of DIN net
264 production with its maximum release at April each year for both of the samples. SO_4^{2-} is
265 dominated by the concentration in the precipitation input with some leaching in the soil and
266 sulphides in the dolomite. Its variability constant is quite low (<0.1). Weighted KGEs, as well
267 as their values for the individual simulation variables are relatively stable. Overall, calibration
268 on both samples provided similar parameter values. Due to its higher stability concerning the
269 evaluation period, we chose the 2nd sample for further analysis.

Formatiert: Nicht Hervorheben

270 The discharge simulations follow adequately the variations of the observations (Figure 4), although some small events are not reproduced by the model and although the simulations
271 of the weir's discharge tend to under-estimate peak flows. No obvious differences can be seen
272 between the pre-disturbance and wind disturbance period. The hydrochemical simulations tend
273 to follow the observations, as well (Figure 5). But there is sometimes some under-
274 estimation of the DOC peaks for the pre-disturbance period. The DIN simulations appear to be
275 more precise during the pre-disturbance period but there is a systematic under-estimation when
276 the disturbance takes place.
277

278 4.2 Model performance during the wind disturbance period

279 There is a deviation between pre-disturbance and disturbance period simulated and observed
280 variability and bias for DIN (Figure 6). A similar tendency can be found for DOC. But
281 only for DIN the deviations are different to the variations already found during the pre-
282 disturbance period (which is also the calibration/validation period). The variations of DOC
283 appear to be systematic, too, but they fall within its ranges of variability during the pre-
284 disturbance period.

285 4.3 Adaption of N parameters for the wind disturbance period

286 The very first signs of the impact were found at May 1st 2007 lasting to the end of the
287 hydrological year 2010/11. In a first trial (Table 2), the model parameters for the DIN
288 production were adapted manually to compensate for the changes of observed DIN
289 concentrations with focus on reducing the difference indicated by the bias β and variability α
290 components of the KGE_{DIN} . In a second trial, we use an automatic calibration scheme to achieve
291 the optimum KGE_{DIN} . As indicated by the highest KGE (Table 2), the automatic
292 calibration provided the highest KGE_{DIN} . But this is achieved by improving variability α and
293 correlation r . Almost no improvement is reached for the bias β . Even though resulting in a
294 slightly lower improvement of KGE_{DIN} the manual calibration results in a much more
295 acceptable reduction of the bias (Figure 6). Its parameter values showed an production
296 rate equilibrium concentration P_{DIN} of DIN more than two times 2 mg/l than the pre-disturbance
297 value, an amplitude A_{DIN} more than 4 times larger, and a phase shift $S_{PH,DIN}$ towards a week
298 earlier in the year, resulting in a more acceptable simulation of DIN dynamics during the
299 disturbance period (Figure 7).

300 4.4 Transit time distributions

301 The transit time distributions show that the soil and epikarst system reacts quite rapidly to the
302 virtual injection. 50% of the injection concentration is reached within ~60 days (Figure 8a),
303 while most of groundwater system requires ~100 days to reach 50% of the injection
304 concentration with few flow paths reach up to 300 days (Figure 8c). A similar
305 behaviour is found when the impact ends (Figure 8bd). It also shows that some of the
306 slowest flow paths just reach the input concentration before they start to decline again.

307 5 Discussion

308 5.1 Reliability of calibrated parameters and model simulations

309 Most of the calibrated model parameters are in ranges that are in accordance with other
310 modelling studies or field evidence. General differences between the calibrated parameter
311 values of the both-sided split sample test may mostly be due to the comparatively low resolution
312 of the hydrochemical variables (SO₄, DOC and DIN) that even increased by the bootstrapping
313 procedure. However, the good multi-objective simulation performance of the model, as well as
314 its evaluation by the split sample test an overall acceptable performance of the model. With
315 almost 3-8 days the epikarst storage constant is in accordance with field studies on the epikarst
316 storage behaviour that found retention times of some days to few weeks (Aquilina et al., 2006;
317 Perrin et al., 2003). The soil as well as the epikarst storage capacity are quite large. These high
318 values may be explained by structural errors of the model that result in unrealistic calibrated
319 parameter values, in particular possible parameter interactions between their storage capacities
320 and storage coefficients. However, the good multi-objective simulation performance of the
321 model, as well as its evaluation by parameter identifiability analysis and the split sample test
322 rather indicate that the overall performance of the model is acceptable. Since the soil and the
323 vegetation controls the fraction of rain that is lost to evapotranspiration this high calibrated
324 value might be due to tree roots ranging through the soil into the epikarst (Heilman et al., 2012)
325 or rock debris (Hartmann et al., 2012a).

326 Similar to the epikarst storage constant, the conduit storage constant, K_C , is, with its value of
327 1.1 days, in the range of previous modelling studies (Fleury et al., 2007; Hartmann et al.,
328 2013a). The high values of the epikarst variability constant and the groundwater constant
329 indicate a low development of preferential flow paths in the rock, which is typical for dolomite
330 aquifers (Ford and Williams, 2007). A low degree of karstification was already known for our

331 study site (Jost et al., 2010) and the calibrated recharge areas fall well into the ranges found in
332 previous modelling studies (Hartmann et al., 2012a, 2013c).

333 The hydrochemical parameters mostly show realistic values. A DOC production parameter
334 *P_{DOC} of ~1.6-1.8 mg/l resulted in realistic simulated concentrations at the weir*~~The production~~
335 *of DOC of ~1.6-1.8 mg/l is in a realistic range.* For DIN production the two calibration
336 samples result in values of -1.4 and 0.1 mg/l, going along with amplitudes of 3.4 and 1.8,
337 respectively. Hence, there appears to be some correlation between the production and amplitude
338 parameters, P_{DIN} and A_{DIN} . Negative values indicate that during some periods of the year all
339 *DIN is consumed by plants or soil organisms*~~For a negative mean DIN production, and that the~~
340 production period ~~would be~~ shorter, but more pronounced due to its larger value of amplitude.
341 But we expect these differences to be minor since the phase shift $S_{PH,DIN}$ of both calibration
342 samples is almost the same, as well as their annual maximum ($P_{DIN} + A_{DIN}$) of 2.01 mg/l and
343 1.95 mg/l. It indicates a maximum of DIN production and leaching at the time of the year when
344 snow melt reaches its maximum (March to April) and when DIN uptake by plants is still low
345 (Jost et al., 2010). The dissolution equilibrium concentrations of 2.7-3.1 mg/l for SO_4^{2-} indicate
346 the abundance of the precipitation-input, oxidation of sulphides (e.g. pyrite) in the dolomite and
347 traces of evaporates in the small Plattenkalk occurrences (Kralik et al., 2006).

348 5.2 Impact of storms

349 The deviation between simulated and observed time series (~~Figure 5~~Figure 5) already indicates
350 that DIN is the only solute that shows a clear impact of the storms. This is further corroborated
351 by considering the individual components of KGE in ~~Figure 6~~Figure 6. It is well known that
352 nitrate leaching to the groundwater increases sharply after tree damage (dieback) in forests
353 where N is not strongly limited (Bernal et al., 2012; Griffin et al., 2011; Huber, 2005). Such
354 disturbances disrupt the N cycle. The loss of tree N uptake favours nitrification of surplus NH_4^+
355 by microorganism. Moreover, above- (i.e. foliage) and belowground (i.e. fine roots) litter from
356 dead trees enhances the mineralization of organic matter, ammonification and nitrification.
357 Both processes are accelerated by increased soil moisture and soil temperature due to the loss
358 of the forest canopy. -Subsequently, leaching of N increases with increased seepage fluxes due
359 to decreased interception and water uptake by trees. Since the simple DIN routine of the model
360 cannot take into account such changes the under-estimated DIN concentrations and their
361 amplitude show the effect of forest disturbance on the leaching of DIN from the studied

Formatiert: Englisch (Großbritannien)

Formatiert: Schriftart: Kursiv, Englisch (Großbritannien)

Formatiert: Schriftart: Kursiv, Englisch (Großbritannien),
Tiefgestellt

Formatiert: Englisch (Großbritannien)

Formatiert: Englisch (Großbritannien)

362 catchment. There is also an apparently systematic deviation of the DOC variability α . But its
363 variations during the pre-storm period are similarly large and thus points to a negligible effect
364 of forest disturbance on DOC leaching. Numerous studies identified the forest floor as DOC
365 source (Borken et al., 2011; Michalzik et al., 2001). Windthrow generally causes a (short-term)
366 pulse of above- and belowground litter (Harmon et al., 2011). Thereby, mineralization of the
367 surplus litter input concurrent with improved soil climatic conditions likely increased the
368 leaching of DOC from the forest floor (Fröberg et al., 2007; Kalbitz et al., 2007). Concurrent,
369 increased soil water, surface and shallow subsurface flow may favour increased soil DOC
370 leaching to downslope surface waters (Monteith et al., 2006; Neff and Asner, 2001; Sanderman
371 et al., 2009). In mountainous catchment the latter flow paths are likely due to the steepness of
372 the catchment slopes (Boyer et al., 1997; Sakamoto et al., 1999; Terajima and Moriizumi,
373 2013). The missing signal of forest disturbance on DOC concentrations at the weir 1 even
374 shortly after the disturbance may be due to the minor extension of the disturbed area, the minor
375 increase of surface and shallow subsurface flow due to the relative low slope of the disturbed
376 area, the buffering of increased topsoil DOC leaching due to absorption of DOC within the
377 subsoil (Borken et al., 2011; Huber et al., 2004), missing DOC-rich riparian source areas (i.e.
378 wetlands, floodplains) and the reduction pre-disturbance organic matter input to soil (i.e. litter,
379 root exudates) (Högberg and Högberg, 2002). Theoretically, hydrological processes such as a
380 decrease of transpiration or an increase of groundwater recharge may also occur. But these
381 superficial changes are probably minor considering the typically high karstic infiltration
382 capacities that remove surface water quite rapidly (Hartmann et al., 2014b, 2015). For both,
383 disturbance induced changes of DOC and hydrological processes, more sampling in high
384 temporal-resolution should be undertaken to elucidate the effect of forest disturbance within
385 the studied ecosystem.

386 **5.2.1 N leaching from the soil**

387 Adapting the DIN solute transport parameters by an automatic calibration scheme resulted in
388 an increased KGE_{DIN} (Figure 7~~Figure 7~~). But it did not resolve the bias of simulated and
389 observed DIN concentrations during the wind disturbance period since the overall improvement
390 of KGE_{DIN} was reached by an improvement of r and α (Table 2~~Table 2~~). Adjusting the DIN
391 parameters manually resulted in a more acceptable decrease of the bias β that also went along
392 with an increase of the overall KGE_{DIN} . An increase of the DIN production rate equilibrium
393 concentration of ~ 2 mg/l indicates a massive mobilisation of DIN and a reduction of its

394 seasonal amplitude by ~1.1 mg/l. Even though there may be some correlation between mean
395 annual production and amplitude (see previous section), the annual maximum of 2.80 mg/l
396 ($P_{DIN} + A_{DIN}$) indicates an increase of the DIN concentrations in the soil of at least ~0.8 mg/l
397 (from 1.95 to 2.01 mg/l at the pre-disturbance period).

398 We identified the beginning of the impact at May 1st 2007 and its end by the end of the
399 hydrological year 2010/11. This is more than 2 years after the last storm in 2008 indicates how
400 long the ecosystem takes to recover from the disturbance. Other studies have shown comparable
401 recovery times (Katzensteiner, 2003; Weis et al., 2006) or longer (Huber, 2005). Considering
402 the deviations between DIN simulations by the pre-disturbance calibration and the DIN
403 simulations obtained by the manual adjustment, they sum up to an additional release of 9.9
404 kg/ha of DIN over the whole period of ~3.7 years, or 2.7 kg/ha/a in addition to 5.8 kg/ha/a that
405 would have been released without the wind disturbance. These values only corresponds to
406 inorganic N. Other studies showed that also dissolved organic N can contribute to vertical
407 percolation but only in small ratios from 2-5% (Solinger et al., 2001; Wu et al., 2009). The
408 apparent shift of $S_{PH,DIN}$ towards an earlier maximum of DIN release (7 days) may probably be
409 due to the earlier onset of snow melt in open areas as compared to forests because snow melt is
410 a major driver of DIN leaching from the soils in our study area (Jost et al., 2010).

411 **5.2.2 N propagation through the hydrological system**

412 The virtual tracer injections that we applied with the beginning of the disturbance period
413 elaborate the hydrological system's filter and retardation capacity. Due to their higher dynamics
414 the soil and the epikarst system adapt more rapidly to the change within weeks and months.
415 Similar behaviour was also found in previous studies (Hartmann et al., 2012a; Kralik et al.,
416 2009). ~~But the groundwater system takes much longer. Even though~~ The majority of the
417 simulated flow paths adapts to the virtual tracer signal within a few months, which is in
418 accordance with water isotope studies as the weir (Humer and Kralik, 2008; Kralik et al., 2009).
419 However, using age dating (CFC and SF6) and artificial tracer experiments at individual springs
420 within the study area, the Kralik et al. (Kralik et al., 2009) also found ages from several days to
421 several decades. Hence, the majority of transit times found by the virtual tracer experiment
422 reflect the average behaviour of the sub-catchment drained by the weir, which can be regarded
423 as more dominant than observations at individual the springs that rather represent fast and slow
424 flow paths of minor importance. -some of them need years to approach the virtual tracer's
425 concentration. Such slow pathways were also identified by water age dating analysis that found

Feldfunktion geändert

Formatiert: Deutsch (Deutschland)

426 ~~water ages of up to 22 years (Humer and Kralik, 2008; Kralik et al., 2009).~~ The retardation is
427 also visible from the dynamics of the DIN concentrations just after the end of the disturbance
428 period (beginning of 2011/12, ~~Figure 7~~Figure 7). Even though DIN production is set to pre-
429 disturbance conditions, it almost takes 4 months for the DIN simulations (by manual
430 calibration) to adopt to their undisturbed concentrations (pre-disturbance calibration). Due to
431 their small contribution (<5%), the slower flow paths do not have a significant impact on the
432 retardation capacity of the hydrological system.

433 5.3 Implications

434 Our results corroborate findings from many other studies that extreme events as during the wind
435 disturbance period in our study can result in significant increase of DIN in the runoff, despite
436 the area impacted was relative small (5-10% of the watershed). Particularly in karst catchments
437 such changes can happen quickly and prevail for a significant duration, in our case more than
438 2 years after the last storm. Due to subsurface heterogeneity the impact did not travel uniformly
439 through the system. It rather split into different pathways and mixed with old water that
440 percolated prior to the impact. In our system, large parts of the water travelled rapidly through
441 the system. But a smaller number of pathways had large storages of old water and slow flow
442 velocities resulting in significant retardation. Taking into account that forest disturbances will
443 most probably increase with climate change (Seidl et al., 2014), DIN mobilisation as observed
444 in our study may occur more often and more intense. The hydrological system may dilute and
445 delay rapid shifts of N concentration, and it will “memorize” the impacts for some time. But
446 our present analysis showed that the time scale of the wind disturbance on DIN production and
447 leaching from the soil exceeds the time scale of transit of the disturbance through the system.
448 This is most probably due to the small size and the subsurface karstic behaviour of our study
449 site that favours faster flow paths and low system storage than hydrological systems with larger
450 extent or with other types of geology.

451 6 Conclusions

452 In our study we used a process-based semi distributed karst model to simulate DOC, DIN and
453 SO_4^{2-} transport through a dolomite karst system in Austria. We calibrated and validated our
454 model during a 4-year time period just before a series of heavy storms caused strong wind
455 disturbance to the study site' ecosystem. To quantify its impact we run the model for the entire
456 disturbance period using the parameters we found at the pre-storm period. The deviations

457 between the simulations and the observations gave us indication that there was a significant
458 shift in DIN mobilisation, its seasonal amplitude and its timing. Estimating the beginning and
459 end of the disturbance period we applied a continuous virtual tracer injection to obtain the mean
460 transit times of the karst system. They showed us how the hydrological system filtered and
461 retarded the impact of the disturbance at the system outlet.

462 Even though our study is only considering one site and one wind disturbance period it already
463 provides some generally applicable conclusions: (1) hydroclimatic extremes such as storms do
464 not only create droughts or floods; they can also affect water quality; (2) a hydrological system
465 can filter and delay surface impacts but it may also memorize past impacts but only at a limited
466 time scale; (3) water quality models that have been calibrated without consideration of such
467 external impacts will provide poor predictions. For these reasons we believe that future large-
468 scale simulations of water resources have to include water quality simulations that take into
469 account the impact of ecosystem disturbances. Even without anthropogenic contamination
470 climate change will strongly affect water quality in our aquifers and streams and we have to
471 understand and prepare ourselves to avoid threats on future water supply.

472 **7 Acknowledgements**

473 Financial support by the Transnational Access to Research Infrastructures activity in the 7th
474 Framework Programme of the EC under the ExpeER project and the South East Europe
475 Transnational Cooperation Programme OrientGate for conducting the research is gratefully
476 acknowledged. This work was supported by a fellowship within the Postdoc Programme of the
477 German Academic Exchange Service (DAAD).

478 **8 Appendix**

479 The variability of soil depths in the model is expressed by a mean soil depth $V_{mean,S}$ [mm] and
480 a distribution coefficient a_{SE} [-]. The soil storage capacity $V_{S,i}$ [mm] for every compartment i is
481 calculated by:

$$482 \quad V_{S,i} = (1 - f_{var,S}) \cdot V_{mean,S} + V_{max,S} \cdot \left(\frac{i}{Z}\right)^{a_{SE}} \quad (7)$$

483 Where the maximum soil storage capacity $V_{max,S}$ [mm] is derived from $(f_{var,S} \cdot V_{mean,S})$ as
484 described in Hartmann et al. (2013c). $f_{var,S}$ [-] is the fraction of the soil that shows variable
485 thicknesses while $(1 - f_{var,S})$ has uniform value. The same distribution coefficient a_{SE} is used to

486 define the epikarst storage distribution by the mean epikarst depth $V_{mean,E}$ [mm] (derivation of
 487 $V_{max,E}$ identical to $V_{mean,S}$):

$$488 \quad V_{E,i} = V_{max,E} \cdot \left(\frac{i}{Z}\right)^{a_{SE}} \quad (8)$$

489 Actual evapotranspiration from each soil compartment at time step t $E_{act,i}$ is found by:

$$490 \quad E_{act,i}(t) = E_{pot}(t) \cdot \frac{\min[V_{Soil,i}(t) + P(t) + Q_{Surface,i}(t), V_{S,i}]}{V_{S,i}} \quad (9)$$

491 where $Q_{Surface,i}$ [mm/d] is the surface inflow originating from compartment $i-1$ (see Eq. (13)),
 492 E_{pot} [mm/d] the potential evaporation, and P [mm/d] the precipitation at time t . E_{pot} is calculated
 493 by the Penman-Wendling approach (Wendling et al., 1991; DVWK, 1996). To account for the
 494 solid fraction of precipitation a snowmelt routine was set on top of the model. We used the
 495 same routine that was applied on 148 other catchments in Austria by Parajka et al. (2007) and
 496 explained in Hartmann et al. (2012). Recharge to the epikarst $R_{Epi,i}$ [mm/d] is defined as:

$$497 \quad R_{Epi,i}(t) = \max[V_{Soil,i}(t) + P(t) + Q_{Surface,i}(t) - E_{act,i}(t) - V_{S,i}, 0] \quad (10)$$

498 Where the storage coefficients $K_{E,i}$ [d] control the outflow of the epikarst:

$$499 \quad Q_{Epi,i}(t) = \frac{\min[V_{Epi,i}(t) + R_{Epi,i}(t) + Q_{Surface,i}(t), V_{E,i}]}{K_{E,i}} \cdot \Delta t \quad (11)$$

$$500 \quad K_{E,i} = K_{max,E} \cdot \left(\frac{Z-i+1}{Z}\right)^{a_{SE}} \quad (12)$$

501 $K_{max,E}$ is derived by a mean epikarst storage coefficient $K_{mean,E}$ (see Hartmann et al., 2013c).

502 Excess water from the soil and epikarst that produces surface flow to the next model
 503 compartment $Q_{Surf,i+1}$ [mm/d] is calculated by:

$$504 \quad Q_{Surf,i+1}(t) = \max[V_{Epi,i}(t) + R_{Epi,i}(t) - V_{E,i}, 0] \quad (13)$$

505 The lower outflow of each epikarst compartment is separated into diffuse ($R_{diff,i}$ [mm/d]) and
 506 concentrated groundwater recharge ($R_{conc,i}$ [mm/d]) by the recharge separation factor $f_{C,i}$ [-]:

$$507 \quad R_{conc,i}(t) = f_{C,i} \cdot Q_{Epi,i}(t) \quad (14)$$

$$508 \quad R_{diff,i}(t) = (1 - f_{C,i}) \cdot Q_{Epi,i}(t) \quad (15)$$

509 The distribution of $f_{C,i}$ among the different compartments is defined by the distribution
 510 coefficient a_{fsep} :

$$511 \quad f_{C,i} = \left(\frac{i}{Z}\right)^{a_{fsep}}$$

$$512 \quad (16)$$

513 Diffuse recharge reaches the groundwater compartment below, while concentrated recharge is
 514 routed to the conduit system (compartment $i = Z$). The variable contributions of the
 515 groundwater compartments that represent diffuse flow through the matrix ($1 \dots Z - 1$) are given
 516 by

$$517 \quad Q_{GW,i}(t) = \frac{V_{GW,i}(t) + R_{diff,i}(t)}{K_{GW,i}} \quad (17)$$

518 $K_{GW,i}$ is calculated by:

$$519 \quad K_{GW,i} = K_C \cdot \left(\frac{Z-i+1}{Z}\right)^{-a_{GW}} \quad (18)$$

520 where K_C is the conduit storage coefficient. The groundwater contribution of the conduit system
 521 originates from compartment Z :

$$522 \quad Q_{GW,Z}(t) = \frac{\min \left[V_{GW,Z}(t) + \sum_{i=1}^Z R_{conc,i}(t), V_{crit,OF} \right]}{K_C} \quad (19)$$

523 Knowing the recharge area A_{max} [km^2] and rescaling the dimensions [l s^{-1}], the discharge of the
 524 entire system Q [l s^{-1}] is calculated by:

$$525 \quad Q(t) = \frac{A_{max}}{Z} \cdot \sum_{i=1}^Z Q_{GW,i}(t) \quad (20)$$

526

527 9 References

528 [Andreo, B., Ravbar, N. and Vías, J. M.: Source vulnerability mapping in carbonate \(karst\)](#)
 529 [aquifers by extension of the COP method: application to pilot sites, Hydrogeol. J., 17\(3\), 749–](#)
 530 [758, doi:10.1007/s10040-008-0391-1, 2008.](#)

531 [Aquilina, L., Ladouche, B. and Doerfliger, N.: Water storage and transfer in the epikarst of](#)

Feldfunktion geändert

Formatiert: Englisch (USA)

532 karstic systems during high flow periods, *J. Hydrol.*, 327, 472–485, 2006.

533 Bakalowicz, M.: Karst groundwater: a challenge for new resources, *Hydrogeol. J.*, 13, 148–
534 160, 2005.

535 Bernal, S., Hedin, L. O., Likens, G. E., Gerber, S. and Buso, D. C.: Complex response of the
536 forest nitrogen cycle to climate change, , doi:10.1073/pnas.1121448109/-
537 /DCSupplemental.www.pnas.org/cgi/doi/10.1073/pnas.1121448109, 2012.

538 Beven, K. J.: A manifesto for the equifinality thesis, *J. Hydrol.*, 320(1-2), 18–36 [online]
539 Available from: [http://www.sciencedirect.com/science/article/B6V6C-4H16S4M-
540 1/2/571c8821621c803522cc823147bef169](http://www.sciencedirect.com/science/article/B6V6C-4H16S4M-1/2/571c8821621c803522cc823147bef169), 2006.

541 Borken, W., Ahrens, B., Schulz, C. and Zimmermann, L.: Site-to-site variability and temporal
542 trends of DOC concentrations and fluxes in temperate forest soils, *Glob. Chang. Biol.*, 17(7),
543 2428–2443, doi:10.1111/j.1365-2486.2011.02390.x, 2011.

544 Boyer, E. W., Hornberger, G. M., Bencala, K. E. and McKnight, D. M.: Response
545 characteristics of DOC flushing in an alpine catchment, *Hydrol. Process.*, 11(12), 1635–1647,
546 doi:10.1002/(SICI)1099-1085(19971015)11:12<1635::AID-HYP494>3.0.CO;2-H, 1997.

547 Butscher, C. and Huggenberger, P.: Intrinsic vulnerability assessment in karst areas: A
548 numerical modeling approach, *Water Resour. Res.*, 44, W03408, doi:10.1029/2007WR006277,
549 2008.

550 Butterbach-Bahl, K., Gundersen, P., Ambus, P., Augustin, J., Beier, C., Boeckx, P.,
551 Dannenmann, M., Sanchez Gimeno, B., Ibrom, A. and Kiese, R.: Nitrogen processes in
552 terrestrial ecosystems, *Eur. nitrogen Assess. sources, Eff. policy Perspect.*, 99–125, 2011.

553 Charlier, J.-B., Bertrand, C. and Mudry, J.: Conceptual hydrogeological model of flow and
554 transport of dissolved organic carbon in a small Jura karst system, *J. Hydrol.*, 460-461, 52–64,
555 doi:10.1016/j.jhydrol.2012.06.043, 2012.

556 Christensen, J. H., Hewitson, B., Busuioc, A., Chen, A., Gao, X., Held, I., Jones, R., Kolli, R.
557 K., Kwon, W.-T., Laprise, R., Rueda, V. M., Mearns, L., Menéndez, C. G., Räisänen, J., Rinke,
558 A., Sarr, A. and Whetton, P.: Regional Climate Projections, in *Climate Change 2007: The
559 Physical Science Basis. Contribution of Working Group I to the Fourth Assessment Report of
560 the Intergovernmental Panel on Climate Change*, edited by S. Solomon, D. Qin, M. Manning,
561 Z. Chen, M. Marquis, K. B. Averyt, M. Tignor, and H. L. Miller, p. 996, Cambridge University
562 Press, Cambridge, United Kingdom and New York, NY, USA. [online] Available from:
563 [http://www.ipcc.ch/publications_and_data/publications_ipcc_fourth_assessment_report_wg1_
564 report_the_physical_science_basis.htm](http://www.ipcc.ch/publications_and_data/publications_ipcc_fourth_assessment_report_wg1_report_the_physical_science_basis.htm), 2007.

565 COST: COST 65: Hydrogeological aspects of groundwater protection in karstic areas, Final
566 report (COST action 65), edited by D.-G. X. I. I. S. European Commission Research and
567 Development, *Eur. Comm. Dir. XII Sci. Res. Dev.*, Report EUR, 446, 1995.

568 Dai, A.: Increasing drought under global warming in observations and models, *Nat. Clim.*
569 *Chang.*, 3(1), 52–58, doi:10.1038/nclimate1633, 2012.

570 Doerfliger, N., Jeannin, P.-Y. and Zwahlen, F.: Water vulnerability assessment in karst
571 environments: a new method of defining protection areas using a multi-attribute approach and
572 GIS tools (EPIK method), *Environ. Geol.*, 39(2), 165–176, 1999.

573 Einsiedl, F., Maloszewski, P. and Stichler, W.: Estimation of denitrification potential in a karst
574 aquifer using the 15N and 18O isotopes of NO₃⁻, *Biogeochemistry*, 72(1), 67–86 [online]
575 Available from: <http://dx.doi.org/10.1007/s10533-004-0375-8>, 2005.

576 Erisman, J. W. and Vries, W. de: Nitrogen deposition and effects on European forests, *Environ.*
577 *Rev.*, 8(2), 65–93, doi:10.1139/a00-006, 2000.

578 Fenicia, F., Kavetski, D., Savenije, H. H. G., Clark, M. P., Schoups, G., Pfister, L. and Freer,
579 J.: Catchment properties, function, and conceptual model representation: is there a
580 correspondence?, *Hydrol. Process.*, 28, 2451–2467, doi:10.1002/hyp.9726, 2014.

581 Feyen, L., Vrugt, J. a., Nualláin, B. Ó., van der Knijff, J. and De Roo, A.: Parameter
582 optimisation and uncertainty assessment for large-scale streamflow simulation with the
583 LISFLOOD model, *J. Hydrol.*, 332(3-4), 276–289, doi:10.1016/j.jhydrol.2006.07.004, 2007.

584 Fleury, P., Plagnes, V. and Bakalowicz, M.: Modelling of the functioning of karst aquifers with
585 a reservoir model: Application to Fontaine de Vaucluse (South of France), *J. Hydrol.*, 345, 38–
586 49, 2007.

587 Ford, D. C. and Williams, P. W.: *Karst Hydrogeology and Geomorphology*, Wiley, Chichester.,
588 2007.

589 Fröberg, M., Jardine, P. M., Hanson, P. J., Swanston, C. W., Todd, D. E., Tarver, J. R. and
590 Garten, C. T.: Low Dissolved Organic Carbon Input from Fresh Litter to Deep Mineral Soils,
591 *Soil Sci. Soc. Am. J.*, 71(2), 347, doi:10.2136/sssaj2006.0188, 2007.

592 Goldscheider, N. and Drew, D.: *Methods in Karst Hydrogeology*, edited by I. A. of
593 Hydrogeologists, Taylor & Francis Group, Leiden, NL., 2007.

594 Gough, R., Holliman, P. J., Heard, T. R. and Freeman, C.: Dissolved organic carbon and
595 trihalomethane formation potential removal during coagulation of a typical UK upland water
596 with alum, PAX-18 and PIX-322, *J. Water Supply Res. Technol.*, 63(8), 650–660, 2014.

597 Griffin, J. M., Turner, M. G. and Simard, M.: Nitrogen cycling following mountain pine beetle
598 disturbance in lodgepole pine forests of Greater Yellowstone, *For. Ecol. Manage.*, 261(6),
599 1077–1089, doi:10.1016/j.foreco.2010.12.031, 2011.

600 Gundersen, P., Schmidt, I. K. and Raulund-Rasmussen, K.: Leaching of nitrate from temperate
601 forests – effects of air pollution and forest management, *Environ. Rev.*, 14(1), 1–57,
602 doi:10.1139/a05-015, 2006.

603 Gupta, H. V, Kling, H., Yilmaz, K. K. and Martinez, G. F.: Decomposition of the mean squared

Formatiert: Englisch (Großbritannien)

Formatiert: Englisch (USA)

604 error and NSE performance criteria: Implications for improving hydrological modelling, *J.*
605 *Hydrol.*, 377(1-2), 80–91, doi:10.1016/j.jhydrol.2009.08.003, 2009.

606 Hagedorn, F., Schleppe, P., Waldner, P. and Flühler, H.: Export of dissolved organic carbon and
607 nitrogen from Gleysol dominated catchments – the significance of water flow paths,
608 *Biogeochemistry*, 50, 137–161, 2000.

609 Harmon, M. E., Bond-Lamberty, B., Tang, J. and Vargas, R.: Heterotrophic respiration in
610 disturbed forests: A review with examples from North America, *J. Geophys. Res.*
611 *Biogeosciences*, 116(2), 1–17, doi:10.1029/2010JG001495, 2011.

612 Hartmann, A., Barberá, J. A., Lange, J., Andreo, B. and Weiler, M.: Progress in the hydrologic
613 simulation of time variant recharge areas of karst systems – Exemplified at a karst spring in
614 Southern Spain, *Adv. Water Resour.*, 54, 149–160, doi:10.1016/j.advwatres.2013.01.010,
615 2013a.

616 Hartmann, A., Gleeson, T., Rosolem, R., Pianosi, F., Wada, Y. and Wagener, T.: A large-scale
617 simulation model to assess karstic groundwater recharge over Europe and the Mediterranean,
618 *Geosci. Model Dev.*, 8(6), 1729–1746, doi:10.5194/gmd-8-1729-2015, 2015.

619 Hartmann, A., Goldscheider, N., Wagener, T., Lange, J. and Weiler, M.: Karst water resources
620 in a changing world: Review of hydrological modeling approaches, *Rev. Geophys.*, 52(3), 218–
621 242, doi:10.1002/2013rg000443, 2014a.

622 Hartmann, A., Kralik, M., Humer, F., Lange, J. and Weiler, M.: Identification of a karst
623 system’s intrinsic hydrodynamic parameters: upscaling from single springs to the whole
624 aquifer, *Environ. Earth Sci.*, 65(8), 2377–2389, doi:10.1007/s12665-011-1033-9, 2012a.

625 Hartmann, A., Lange, J., Weiler, M., Arbel, Y. and Greenbaum, N.: A new approach to model
626 the spatial and temporal variability of recharge to karst aquifers, *Hydrol. Earth Syst. Sci.*, 16(7),
627 2219–2231, doi:10.5194/hess-16-2219-2012, 2012b.

628 Hartmann, A., Mudarra, M., Andreo, B., Marín, A., Wagener, T. and Lange, J.: Modeling
629 spatiotemporal impacts of hydroclimatic extremes on groundwater recharge at a Mediterranean
630 karst aquifer, *Water Resour. Res.*, 50(8), 6507–6521, doi:10.1002/2014WR015685, 2014b.

631 Hartmann, A., Wagener, T., Rimmer, A., Lange, J., Brielmann, H. and Weiler, M.: Testing the
632 realism of model structures to identify karst system processes using water quality and quantity
633 signatures, *Water Resour. Res.*, 49, 3345–3358, doi:10.1002/wrcr.20229, 2013b.

634 Hartmann, A., Weiler, M., Wagener, T., Lange, J., Kralik, M., Humer, F., Mizyed, N., Rimmer,
635 A., Barberá, J. A., Andreo, B., Butscher, C. and Huggenberger, P.: Process-based karst
636 modelling to relate hydrodynamic and hydrochemical characteristics to system properties,
637 *Hydrol. Earth Syst. Sci.*, 17(8), 3305–3321, doi:10.5194/hess-17-3305-2013, 2013c.

638 Heilman, J. L., Litvak, M. E., McInnes, K. J., Kjelgaard, J. F., Kamps, R. H. and Schwinning,
639 S.: Water-storage capacity controls energy partitioning and water use in karst ecosystems on

640 the Edwards Plateau, Texas, *Ecohydrology*, n/a–n/a, doi:10.1002/eco.1327, 2012.

641 Hirabayashi, Y., Mahendran, R., Koirala, S., Konoshima, L., Yamazaki, D., Watanabe, S., Kim,
642 H. and Kanae, S.: Global flood risk under climate change, *Nat. Clim. Chang.*, 3(9), 816–821,
643 doi:10.1038/nclimate1911, 2013.

644 Högberg, M. N. and Högberg, P.: Extramatrical ectomycorrhizal mycelium contributes one-
645 third of microbial biomass and produces, together with associated roots, half the dissolved
646 organic carbon in a forest soil, *New Phytol.*, 154(3), 791–795, doi:10.1046/j.1469-
647 8137.2002.00417.x, 2002.

648 Huber, C.: Long lasting nitrate leaching after bark beetle attack in the highlands of the Bavarian
649 Forest National Park., *J. Environ. Qual.*, 34(5), 1772–9, doi:10.2134/jeq2004.0210, 2005.

650 Huber, C., Baumgarten, M., Göttlein, A. and Rotter, V.: Nitrogen turnover and nitrate leaching
651 after bark beetle attack in mountainous spruce stands of the Bavarian Forest National Park,
652 *Water, Air, Soil Pollut. Focus*, 4(2-3), 391–414, doi:10.1023/B:WAFO.0000028367.69158.8d,
653 2004.

654 Humer, F. and Kralik, M.: Integrated Monitoring Zöbelboden: Hydrologische und
655 hydrochemische Untersuchungen, Unpubl. Rep. Environ. Agency, Vienna, 34, 2008.

656 Johnson, M. S., Billett, M. F., Dinsmore, K. J., Wallin, M., Dyson, K. E. and Jassal, R. S.:
657 Direct and continuous measurement of dissolved carbon dioxide in freshwater aquatic systems
658 — method and applications, , 159(August 2011), 145–159, doi:10.1002/eco, 2010.

659 Jost, G., Dimböck, T., Grabner, M.-T. and Mirtl, M.: Nitrogen Leaching of Two Forest
660 Ecosystems in a Karst Watershed, *Water, Air, & Soil Pollut.*, 218(1-4), 633–649,
661 doi:10.1007/s11270-010-0674-8, 2010.

662 Jourde, H., Mazzilli, N., Lecoq, N., Arfib, B. and Bertin, D.: KARSTMOD: A Generic Modular
663 Reservoir Model Dedicated to Spring Discharge Modeling and Hydrodynamic Analysis in
664 Karst, in *Hydrogeological and Environmental Investigations in Karst Systems SE - 38*, vol. 1,
665 edited by B. Andreo, F. Carrasco, J. J. Durán, P. Jiménez, and J. W. LaMoreaux, pp. 339–344,
666 Springer Berlin Heidelberg., 2015.

667 Kaiser, K. and Kalbitz, K.: Cycling downwards - dissolved organic matter in soils, *Soil Biol.*
668 *Biochem.*, 52, 29–32, doi:10.1016/j.soilbio.2012.04.002, 2012.

669 Kalbitz, K., Meyer, A., Yang, R. and Gerstberger, P.: Response of dissolved organic matter in
670 the forest floor to long-term manipulation of litter and throughfall inputs, *Biogeochemistry*,
671 86(3), 301–318, doi:10.1007/s10533-007-9161-8, 2007.

672 Katz, B. G., Böhlke, J. K. and Hornsby, H. D.: Timescales for nitrate contamination of spring
673 waters, northern Florida, USA, *Chem. Geol.*, 179(1-4), 167–186, 2001.

674 Katz, B. G., Chelette, A. R. and Pratt, T. R.: Use of chemical and isotopic tracers to assess
675 nitrate contamination and ground-water age, Woodville Karst Plain, USA, *J. Hydrol.*, 289(1-

Formatiert: Englisch (USA)

676 4), 36–61, doi:10.1016/j.jhydrol.2003.11.001, 2004.

677 Katzensteiner, K.: Effects of harvesting on nutrient leaching in a Norway spruce (*Picea*, Plant
678 Soil, 250, 59–73, 2003.

679 Kiese, R., Heinzeller, C., Werner, C., Wochele, S., Grote, R. and Butterbach-Bahl, K.:
680 Quantification of nitrate leaching from German forest ecosystems by use of a process oriented
681 biogeochemical model., Environ. Pollut., 159(11), 3204–14,
682 doi:10.1016/j.envpol.2011.05.004, 2011.

683 Klemeš, V.: Dilettantism in Hydrology: Transition or Destiny, Water Resour. Res., 22(9),
684 177S–188S, 1986.

685 Kobler, J., Jandl, R., Dirnböck, T., Mirtl, M. and Schindlbacher, A.: Effects of stand patchiness
686 due to windthrow and bark beetle abatement measures on soil CO₂ efflux and net ecosystem
687 productivity of a managed temperate mountain forest, Eur. J. For. Res., 13, 683–692,
688 doi:10.1007/s10342-015-0882-2, 2015.

689 Kordilla, J., Sauter, M., Reimann, T. and Geyer, T.: Simulation of saturated and unsaturated
690 flow in karst systems at catchment scale using a double continuum approach, Hydrol. Earth
691 Syst. Sci., 16(10), 3909–3923, doi:10.5194/hess-16-3909-2012, 2012.

692 Kralik, M., Humer, F., Grath, J., Numi-Legat, J., Hanus-Illnar, A., Halas, S. and Jelenc, M.:
693 Impact of long distance air pollution on sensitive karst groundwater resources estimated by
694 means of Pb-, S-, O- and Sr-isotopes, in Karst, cambio climático y aguas subterráneas, edited
695 by J. J. Duran, B. Andreo, and F. Carrasco, pp. 311–317, Publicaciones del Instituto Geológico
696 y Minero de España, Serie: Hydrogeología y Aguas Subterráneas N.º 18, Madrid., 2006.

697 Kralik, M., Humer, F., Papesch, W., Tesch, R., Suckow, A., Han, L. F. and Groening, M.:
698 Karstwater-ages in an alpine dolomite catchment , Austria : 18O , 3H , 3H / 3He , CFC and dye
699 tracer investigations, Geophys. Res. Abstr., 11, 11403, European Geosciences Union, General
700 Assembl, 2009.

701 Lindroos, A. J., Derome, J., Mustajärvi, K., Nöjd, P., Beuker, E. and Helmisaari, H. S.: Fluxes
702 of dissolved organic carbon in stand throughfall and percolation water in 12 boreal coniferous
703 stands on mineral soils in Finland, Boreal Environ. Res., 13(SUPPL. B), 22–34, 2008.

704 Löfgren, S., Fröberg, M., Yu, J., Nisell, J. and Ranney, B.: Water chemistry in 179 randomly
705 selected Swedish headwater streams related to forest production, clear-felling and climate,
706 Environ. Monit. Assess., 186(12), 8907–8928, doi:10.1007/s10661-014-4054-5, 2014.

707 Mahler, B. J. and Garner, B. D.: Using Nitrate to Quantify Quick Flow in a Karst Aquifer,
708 Ground Water, 47(3), 350–360 [online] Available from: [http://dx.doi.org/10.1111/j.1745-](http://dx.doi.org/10.1111/j.1745-6584.2008.00499.x)
709 [6584.2008.00499.x](http://dx.doi.org/10.1111/j.1745-6584.2008.00499.x), 2009.

710 Meyer, J. L., Tate, C. M. and Feb, N.: The Effects of Watershed Disturbance on Dissolved
711 Organic Carbon Dynamics of a Stream T H E E F F E C T S O F WATERSHED

712 DISTURBANCE ON DISSOLVED, , 64(1), 33–44, 1983.

713 Michalzik, B., Kalbitz, K., Park, J., Solinger, S. and Matzner, E.: Fluxes and concentrations of
714 dissolved organic carbon and nitrogen—a synthesis for temperate forests, *Biogeochemistry*, 52,
715 173–205 [online] Available from: <http://link.springer.com/article/10.1023/A:1006441620810>,
716 2001.

717 Mikkelsen, K. M., Bearup, L. a., Maxwell, R. M., Stednick, J. D., McCray, J. E. and Sharp, J.
718 O.: Bark beetle infestation impacts on nutrient cycling, water quality and interdependent
719 hydrological effects, *Biogeochemistry*, 115, 1–21, doi:10.1007/s10533-013-9875-8, 2013.

720 Le Moine, N., Andréassian, V. and Mathevet, T.: Confronting surface- and groundwater
721 balances on the La Rochefoucauld-Touvre karstic system (Charente, France), *Water Resour.*
722 *Res.*, 44, W03403, doi:10.1029/2007WR005984, 2008.

723 Monteith, S. S., Buttle, J. M., Hazlett, P. W., Beall, F. D., Semkin, R. G. and Jeffries, D. S.:
724 Paired-basin comparison of hydrologic response in harvested and undisturbed hardwood forests
725 during snowmelt in central Ontario: II. Streamflow sources and groundwater residence times,
726 *Hydrol. Process.*, 20(5), 1117–1136, doi:10.1002/hyp.6073, 2006.

727 Neff, J. C. and Asner, G. P.: Dissolved organic carbon in terrestrial ecosystems: Synthesis and
728 a model, *Ecosystems*, 4(1), 29–48, doi:10.1007/s100210000058, 2001.

729 Perrin, J., Jeannin, P.-Y. and Zwahlen, F.: Epikarst storage in a karst aquifer: a conceptual
730 model based on isotopic data, Milandre test site, Switzerland, *J. Hydrol.*, 279, 106–124, 2003.

731 Pinault, J.-L., Pauwels, H. and Cann, C.: Inverse modeling of the hydrological and the
732 hydrochemical behavior of hydrosystems: Application to nitrate transport and denitrification,
733 *Water Resour. Res.*, 37(8), 2179–2190, 2001.

734 Raymond, P. a. and Saiers, J. E.: Event controlled DOC export from forested watersheds,
735 *Biogeochemistry*, 100(1-3), 197–209, doi:10.1007/s10533-010-9416-7, 2010.

736 Rimmer, A. and Salingar, Y.: Modelling precipitation-streamflow processes in karst basin: The
737 case of the Jordan River sources, Israel, *J. Hydrol.*, 331, 524–542, 2006.

738 Rogora, M., Mosello, R., Arisci, S., Brizzio, M. C., Barbieri, a., Balestrini, R., Waldner, P.,
739 Schmitt, M., Stähli, M., Thimonier, a., Kalina, M., Puxbaum, H., Nickus, U., Ulrich, E. and
740 Probst, a.: An Overview of Atmospheric Deposition Chemistry over the Alps: Present Status
741 and Long-term Trends, *Hydrobiologia*, 562(1), 17–40, doi:10.1007/s10750-005-1803-z, 2006.

742 Sakamoto, T., Takahashi, M., Terajima, T., Nakai, Y. and Matsuura, Y.: Comparison of the
743 effects of rainfall and snowmelt on the carbon discharge of a small, steep, forested watershed
744 in Hokkaido, northern Japan., *Hydrol. Process.*, 13(May 1998), 2301–2314,
745 doi:10.1002/(SICI)1099-1085(199910)13:14/15<2301::AID-HYP876>3.0.CO;2-U, 1999.

746 Sanderman, J., Lohse, K. a., Baldock, J. a. and Amundson, R.: Linking soils and streams:
747 Sources and chemistry of dissolved organic matter in a small coastal watershed, *Water Resour.*

748 Res., 45(3), 1–13, doi:10.1029/2008WR006977, 2009.

749 Seidl, R., Schelhaas, M., Rammer, W. and Verkerk, P. J.: Increasing forest disturbances in
750 Europe and their impact on carbon storage, *Nat. Clim. Chang.*, 4(September), 1–6,
751 doi:10.1038/nclimate2318, 2014.

752 Solinger, S., Kalbitz, K. and Matzner, E.: Controls on the dynamics of dissolved organic carbon
753 and nitrogen in a Central European deciduous forest, *Biogeochem.*, 55, 327–349, 2001.

754 Terajima, T. and Moriizumi, M.: Temporal and spatial changes in dissolved organic carbon
755 concentration and fluorescence intensity of fulvic acid like materials in mountainous headwater
756 catchments, *J. Hydrol.*, 479, 1–12, doi:10.1016/j.jhydrol.2012.10.023, 2013.

757 Tissier, G., Perrette, Y., Dzikowski, M., Poulenard, J., Hobléa, F., Malet, E. and Fanget, B.:
758 Seasonal changes of organic matter quality and quantity at the outlet of a forested karst system
759 (La Roche Saint Alban, French Alps), *J. Hydrol.*, 482, 139–148,
760 doi:10.1016/j.jhydrol.2012.12.045, 2013.

761 Tritz, S., Guinot, V. and Jourde, H.: Modelling the behaviour of a karst system catchment using
762 non-linear hysteretic conceptual model, *J. Hydrol.*, 397(3-4), 250–262,
763 doi:10.1016/j.jhydrol.2010.12.001, 2011.

764 Verstraeten, A., De Vos, B., Neiryneck, J., Roskams, P. and Hens, M.: Impact of air-borne or
765 canopy-derived dissolved organic carbon (DOC) on forest soil solution DOC in Flanders,
766 Belgium, *Atmos. Environ.*, 83, 155–165, doi:10.1016/j.atmosenv.2013.10.058, 2014.

767 Vrugt, J. A., Gupta, H. V., Bouten, W. and Sorooshian, S.: A Shuffled Complex Evolution
768 Metropolis algorithm for optimization and uncertainty assessment of hydrologic model
769 parameters, *Water Resour. Res.*, 39(8), 1201, doi:10.1029/2002WR001642, 2003.

770 Vrugt, J. A., Gupta, H. V., Dekker, S. C., Sorooshian, S., Wagener, T. and Bouten, W.:
771 Application of stochastic parameter optimization to the Sacramento Soil Moisture Accounting
772 model, *J. Hydrol.*, 325(1-4), 288–307, doi:10.1016/j.jhydrol.2005.10.041, 2006.

773 Weis, W., Rotter, V. and Göttlein, A.: Water and element fluxes during the regeneration of
774 Norway spruce with European beech: Effects of shelterwood-cut and clear-cut, *For. Ecol.
775 Manage.*, 224(3), 304–317, doi:10.1016/j.foreco.2005.12.040, 2006.

776 Weishaar, J. L., Aiken, G. R., Bergamaschi, B. A., Fram, M. S., Fujii, R. and Mopper, K.:
777 Evaluation of Specific Ultraviolet Absorbance as an Indicator of the Chemical Composition
778 and Reactivity of Dissolved Organic Carbon, *Environ. Sci. Technol.*, 37(20), 4702–4708,
779 doi:10.1021/es030360x, 2003.

780 WRB: World reference base for soil resources, edited by FAO, IUSS Working Group, Rome.
781 [online] Available from: <http://www.fao.org/ag/agl/agll/wrb/doc/wrb2006final.pdf>, 2006.

782 Wu, H., Peng, C., Moore, T. R., Hua, D., Li, C., Zhu, Q., Peichl, M., Arain, M. a. and Guo, Z.:
783 Modeling dissolved organic carbon in temperate forest soils: TRIPLEX-DOC model

784 development and validation, *Geosci. Model Dev.*, 7(3), 867–881, doi:10.5194/gmd-7-867-
785 2014, 2014.

786 Wu, Y., Clarke, N. and Mulder, J.: Dissolved Organic Nitrogen Concentrations and Ratios of
787 Dissolved Organic Carbon to Dissolved Organic Nitrogen in Throughfall and Soil Waters in
788 Norway Spruce and Scots Pine Forest Stands Throughout Norway, *Water, Air, Soil Pollut.*,
789 210(1-4), 171–186, doi:10.1007/s11270-009-0239-x, 2009.

790

791

Formatiert: Standard

Formatiert: Englisch (USA)

792 **10 Table captions**

793 Table 1: model parameters, description, ranges and calibrated values with *KGE* performances
794 for the calibration and validation samples~~Table 1: model parameters, description, ranges and~~
795 ~~calibrated values with *KGE* performances for the calibration and validation samples~~

796 Table 2: calibrated pre-storm parameters for DIN dynamics and 2 scenrios for adapting it at the
797 stormy period~~Table 2: calibrated pre-storm parameters for DIN dynamics and 2 sexenrios for~~
798 ~~adapting it at the stormy period~~

799 **11 Figure captions**

800 Figure 1: study site and location of measurement devices (Hartmann et al.,
801 2012a;modified).~~Figure 1: study site and location of measurement devices (Hartmann et al.,~~
802 ~~2012a;modified).~~

803 Figure 2: Intra-annual and inter-annual variations of (a) DOC concentrations, (c) DIN
804 concentrations and (e) discharge, and relation between discharge and (b) DOC and (d) DIN
805 before and during the wind disturbance period.~~Figure 2: Intra annual and inter-annual~~
806 ~~variations of (a) DOC concentrations, (c) DIN concentrations and (e) discharge, and relation~~
807 ~~between discharge and (b) DOC and (d) DIN before and during the wind disturbance period.~~

808 Figure 3: Sketch of model structure; it is assumed that discharge and hydrochemistry at the two
809 weirs is composed by different mixtures of diffuse recharge (green), concentrated recharge
810 (red), diffuse groundwater flow (blue) and concentrated groundwater flow (purple)~~Figure 3:~~
811 ~~Sketch of model structure; it is assumed that discharge and hydrochemistry at the two weirs is~~
812 ~~eomposed by different mixtures of diffuse recharge (green), concentrated recharge (red), diffuse~~
813 ~~groundwater flow (blue) and concentrated groundwater flow (purple)~~

814 Figure 4: Observed versus simulated discharges for the entire karst system and weir 1~~Figure 4:~~
815 ~~Observed versus simulated discharges for the entire karst system and weir 1~~Figure 4: Observed~~
816 ~~versus simulated discharges for the entire karst system and weir 1~~Figure 4: Observed versus~~
817 ~~simulated discharges for the entire karst system and weir 1~~Figure 5: Observed versus simulated~~
818 ~~(a) DOC and (b) DIN at weir 1.~~Figure 5: Observed versus simulated (a) DOC and (b) DIN at~~
819 ~~weir 1.~~~~~~~~~~

820 Figure 5: Observed versus simulated (a) DOC and (b) DIN at weir 1.~~Figure 5: Observed versus~~
821 ~~simulated (a) DOC and (b) DIN at weir 1.~~

822 Figure 6: Individual components of the KGE: (a) ratio of simulated and observed variabilities,
823 (b) ratio of simulated and observed average values, and (c) their correlation for the wind
824 disturbance period; for comparison the KGE components and their inter-annual variability are
825 also shown for pre-storm period and after the correction of the DIN production model
826 parameters during the wind period.Figure 6: Individual components of the KGE: (a) ratio of
827 simulated and observed variabilities, (b) ratio of simulated and observed average values, and
828 (c) their correlation for the wind disturbance period; for comparison the KGE components and
829 their inter-annual variability are also shown for pre-storm period and after the correction of the
830 DIN production model parameters during the wind period.

831 Figure 7: Observed and simulated DIN dynamics using the pre-storm parameters (red line), the
832 scenario 1 parameters derived from the deviations assessed by the KGE components (orange
833 line), and the scenario 2 parameters derived by systematic variation (dark red line).Figure 7:
834 Observed and simulated DIN dynamics using the pre-storm parameters (red line), the scenario
835 1 parameters derived from the deviations assessed by the KGE components (dark yellow line),
836 and the scenario 2 parameters derived by systematic variation (green line).

837 Figure 8: Mean transit times for (a) the soil and epikarst and (c) the groundwater storages
838 derived by an infinite virtual tracer injection starting with the beginning of the wind disturbance
839 period, and the reaction of (b) the soil and epikarst, and (d) the groundwater storage as the
840 impact ends.Figure 8: Mean transit times for (a) the soil and epikarst and (c) the groundwater
841 storages derived by an infinite virtual tracer injection starting with the beginning of the wind
842 disturbance period, and the reaction of (b) the soil and epikarst, and (d) the groundwater storage
843 as the impact ends.

844 12 Tables

845 **Table 1: model parameters, description, ranges and calibrated values with KGE performances for the**
846 **calibration and validation samples**

Parameter	Description	Unit	Ranges		Optimized values	
			Lower	Upper	Sample 1	Sample 2
$V_{mean,S}$	Mean soil storage capacity	mm	0	1500	450.18	599.13
$f_{var,S}$	fraction of the soil that has a variable depth	-	0	1	0.06	0.02
$V_{mean,E}$	Mean epikarst storage capacity	mm	0	1500	1495.49	1233.98
α_{SE}	Soil/epikarst depth variability constant	-	0	2	1.69	1.91
$K_{mean,E}$	Epikarst mean storage constant	d	1	50	2.65	8.27
α_{sep}	Recharge separation variability constant	-	0	2	0.88	1.44
K_C	Conduit storage constant	d	1	10	1.37	1.03

α_{GW}	Groundwater variability constant	-	0	2	2.00	1.88
f_{EW}	Fraction of weir discharge originating from the epikarst	-	0	1	0.56	0.72
$f_{WE,conc}$	Fraction of weir discharge originating from the epikarst as concentrated flow	-	0	1	0.57	0.47
$f_{WGW,conc}$	fraction of weir discharge originating from the groundwater as concentrated flow	-	0	1	0.01	0.06
P_{DOC}	DOC production parameter	mg l ⁻¹	0	15	1.79	1.57
α_{DOC}	DOC variability constant	-	0	2	0.92	1.05
P_{DIN}	DIN production parameter	mg l ⁻¹	-5	10	-1.35	0.11
$S_{PH,DIN}$	Phase of annual DIN production	d	0	365	0	2
A_{DIN}	Amplitude of annual DIN production	mg l ⁻¹	0	10	3.36	1.84
$G_{max,SO4}$	Equilibrium concentration of SO ₄ in matrix	mg l ⁻¹	0	50	2.74	3.07
α_{Geo}	Equilibrium concentration variability constant	-	0	2	0.11	0.04
$KGE_{weighted}$	weighted multi-objective model performance	-	0	1	0.56/0.49*	0.52/0.53*
$KGE_{Q,tot}$	model performance for discharge of entire system	-	0	1	0.41/0.33*	0.35/0.42*
$KGE_{Q,W}$	model performance for discharge of weir	-	0	1	0.67/0.62*	0.61/0.66*
KGE_{DOC}	model performance for DOC concentrations	-	0	1	0.38/0.35*	0.43/0.32*
KGE_{DIN}	model performance for NO ₃ concentrations	-	0	1	0.48/0.40*	0.48/0.45*
KGE_{SO4}	model performance for SO ₄ concentrations	-	0	1	0.74/0.62*	0.64/0.65*

847 * calibration/validation with other sample

848

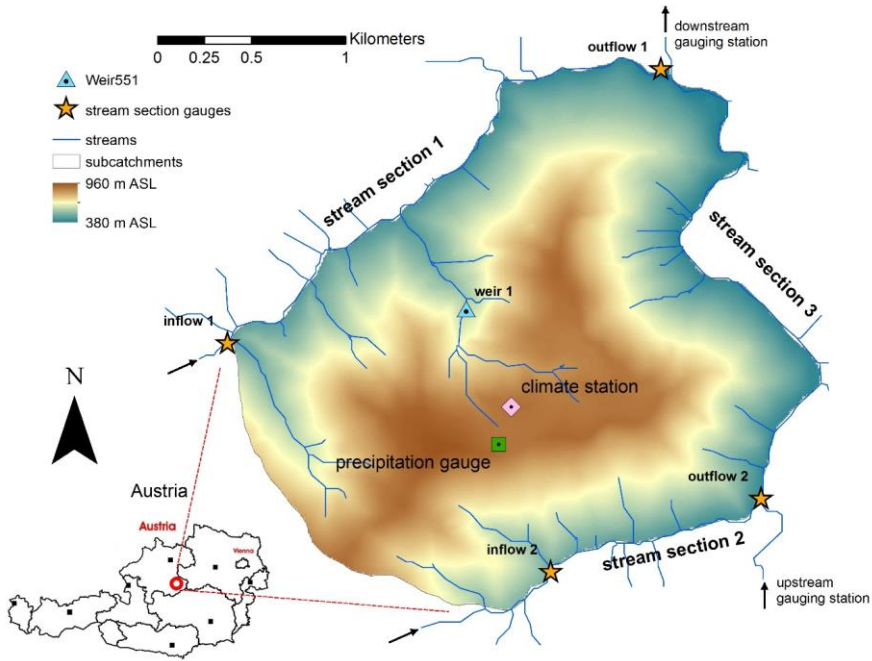
849 **Table 2: calibrated pre-storm parameters for DIN dynamics and 2 scenrios for adapting it at the stormy**
850 **period**

Parameter	Unit	Calibration type		
		Pre-storm	manual	automatic
P_{DIN}	mg l ⁻¹	0.11	2.10	0.00
$S_{PH,DIN}$	d	2.00	9.00	23
A_{DIN}	mg l ⁻¹	1.80	0.70	2.63
KGE_{DIN}^*	-	0.29	0.41	0.46
variability α_{DIN}^*	-	0.75	1.04	1.05
bias β_{DIN}^*	-	0.70	1.01	0.83
correlation DIN^*	-	0.40	0.41	0.49

* for 2006/07-2011/12

851

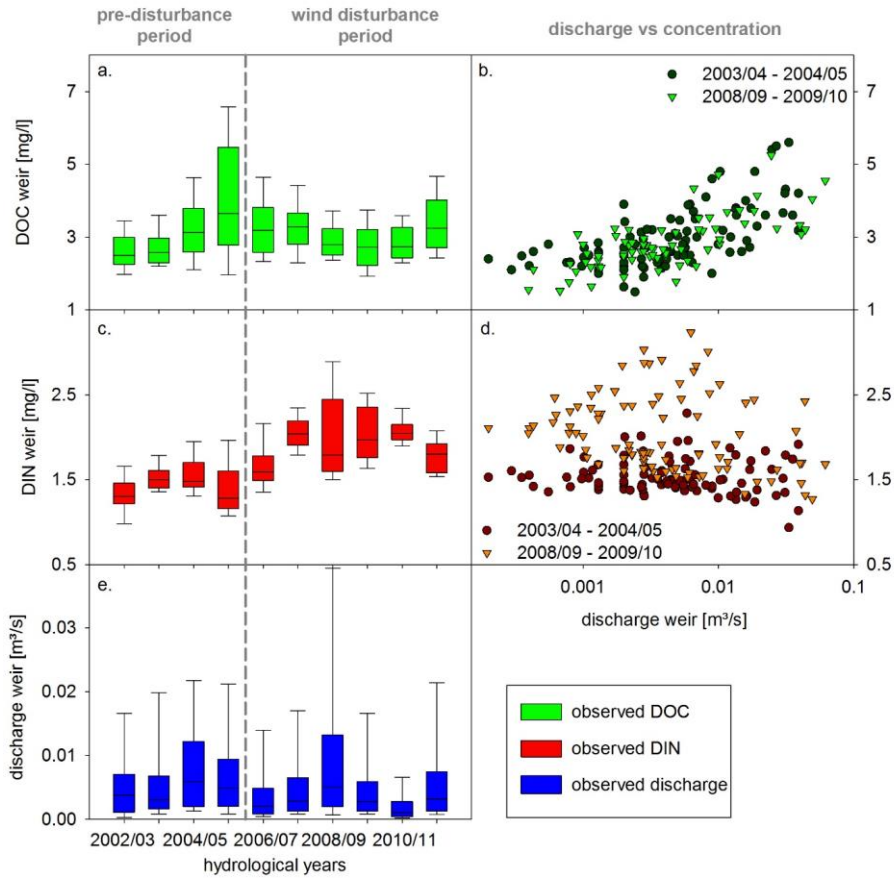
852 13 Figures



853

854 Figure 1: study site and location of measurement devices (Hartmann et al., 2012a;modified).

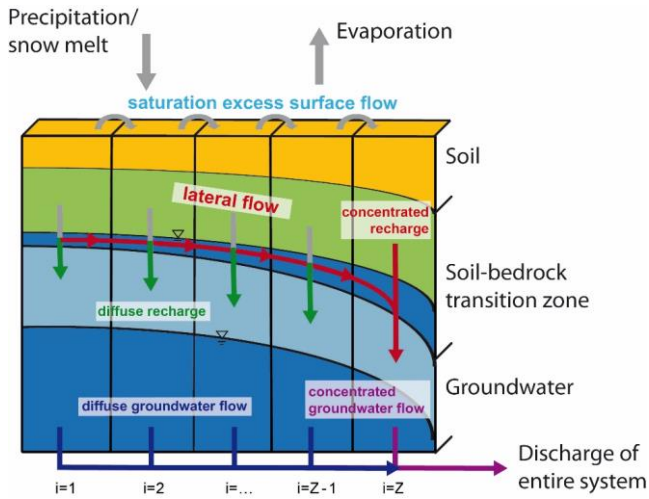
855



856

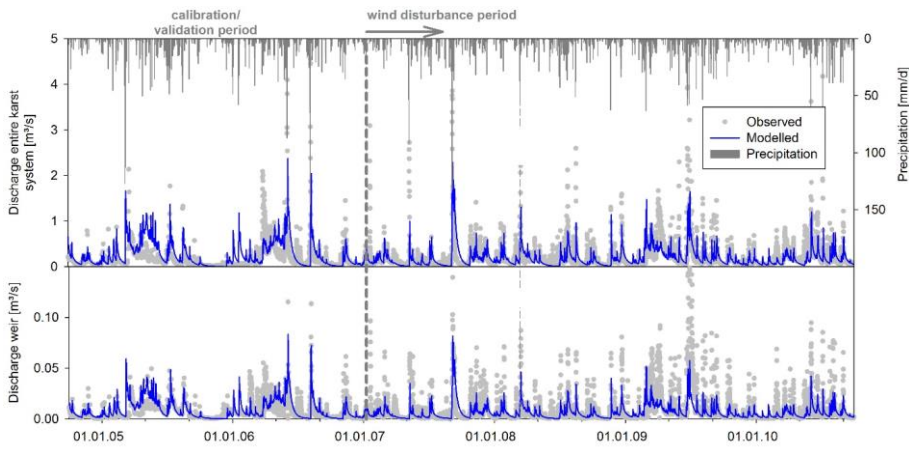
857 **Figure 2: Intra-annual and inter-annual variations of (a) DOC concentrations, (c) DIN concentrations and**
 858 **(e) discharge, and relation between discharge and (b) DOC and (d) DIN before and during the wind**
 859 **disturbance period.**

860



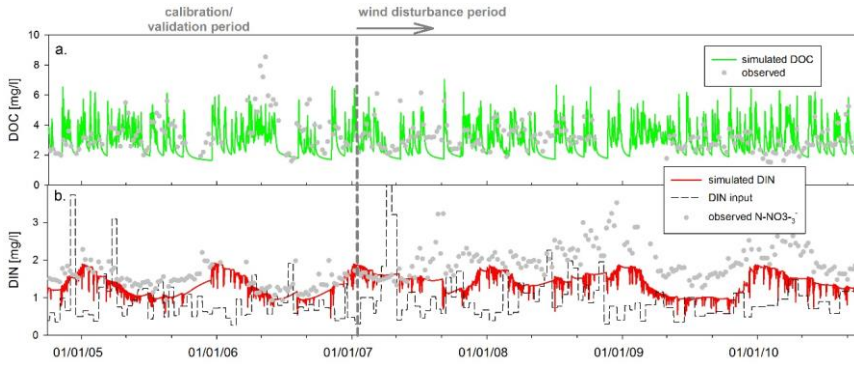
861
 862 **Figure 3: Sketch of model structure; it is assumed that discharge and hydrochemistry at the two weirs is**
 863 **composed by different mixtures of diffuse recharge (green), concentrated recharge (red), diffuse**
 864 **groundwater flow (blue) and concentrated groundwater flow (purple)**

865



866
 867 **Figure 4: Observed versus simulated discharges for the entire karst system and weir 1**

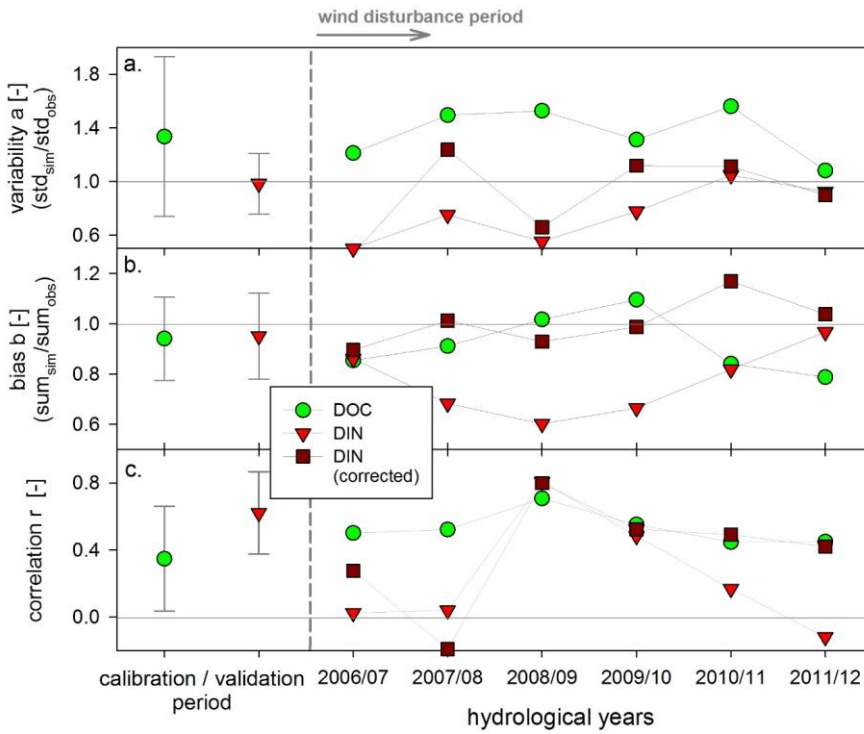
868



869

870 **Figure 5: Observed versus simulated (a) DOC and (b) DIN at weir 1.**

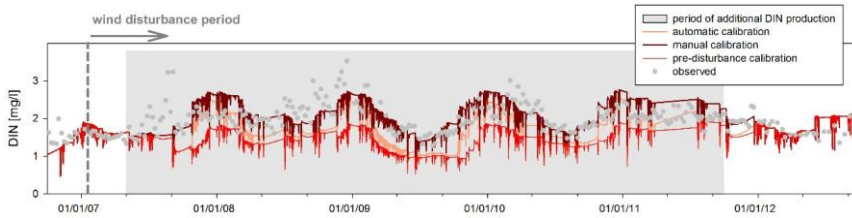
871



872

873 **Figure 6: Individual components of the KGE: (a) ratio of simulated and observed variabilities, (b) ratio of**
 874 **simulated and observed average values, and (c) their correlation for the wind disturbance period; for**
 875 **comparison the KGE components and their inter-annual variability are also shown for pre-storm period**
 876 **and after the correction of the DIN production model parameters during the wind period.**

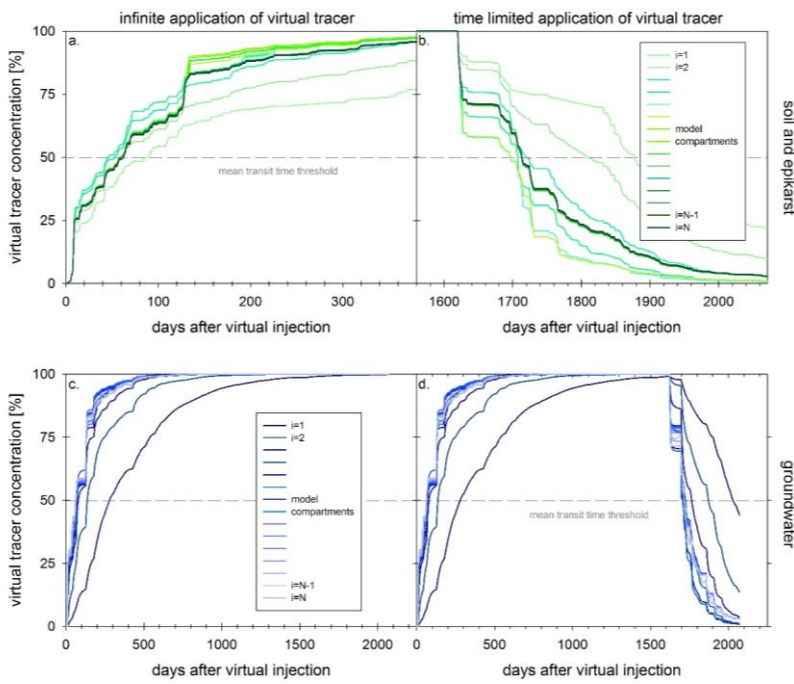
877



878

879 **Figure 7: Observed and simulated DIN dynamics using the pre-storm parameters (red line), the scenario**
880 **1 parameters derived from the deviations assessed by the KGE components (orange line), and the scenario**
881 **2 parameters derived by systematic variation (dark red line).**

882



883

884 **Figure 8: Mean transit times for (a) the soil and epikarst and (c) the groundwater storages derived by an**
885 **infinite virtual tracer injection starting with the beginning of the wind disturbance period, and the**
886 **reaction of (b) the soil and epikarst, and (d) the groundwater storage as the impact ends.**